

# GENERAL THEORY:

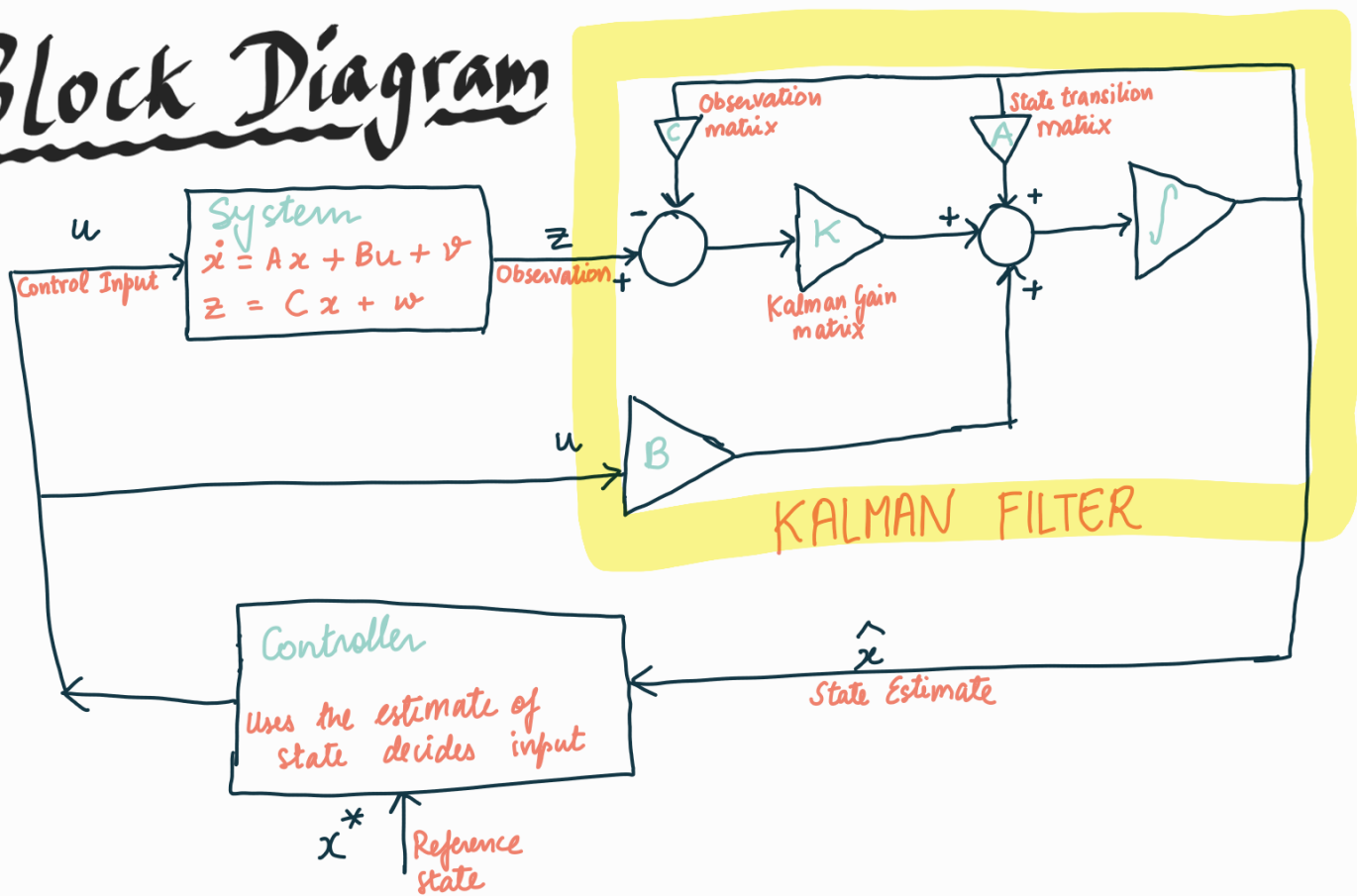
We use the fact that the Kalman filter design process is dual of the LQR design problem.

We minimize :  $\int (x^T Q x + u^T R u) dx$  in the LQR problem.  
(Find  $B$ , s.t.  $u = Bx$ )

For the dual representation, if we solve the problem for the system:

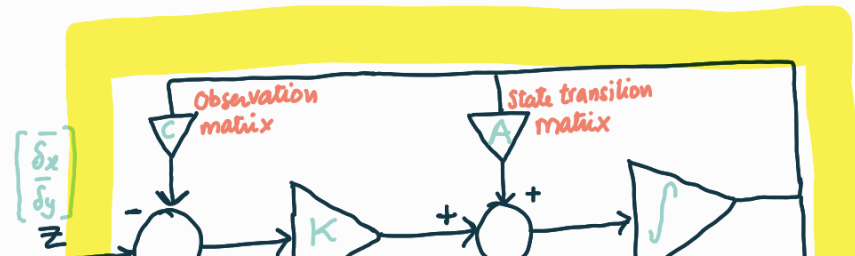
$\dot{x} = A^T x + C^T u$   
 with  $Q$  = Process noise covariance.  $[Q_{ij}] = E [v_i \cdot v_j]$   
 $R$  = Measurement noise covariance.  $[R_{ij}] = E [w_i \cdot w_j]$   
 The optimal  $B$ 's transpose corresponds to Kalman gain matrix.

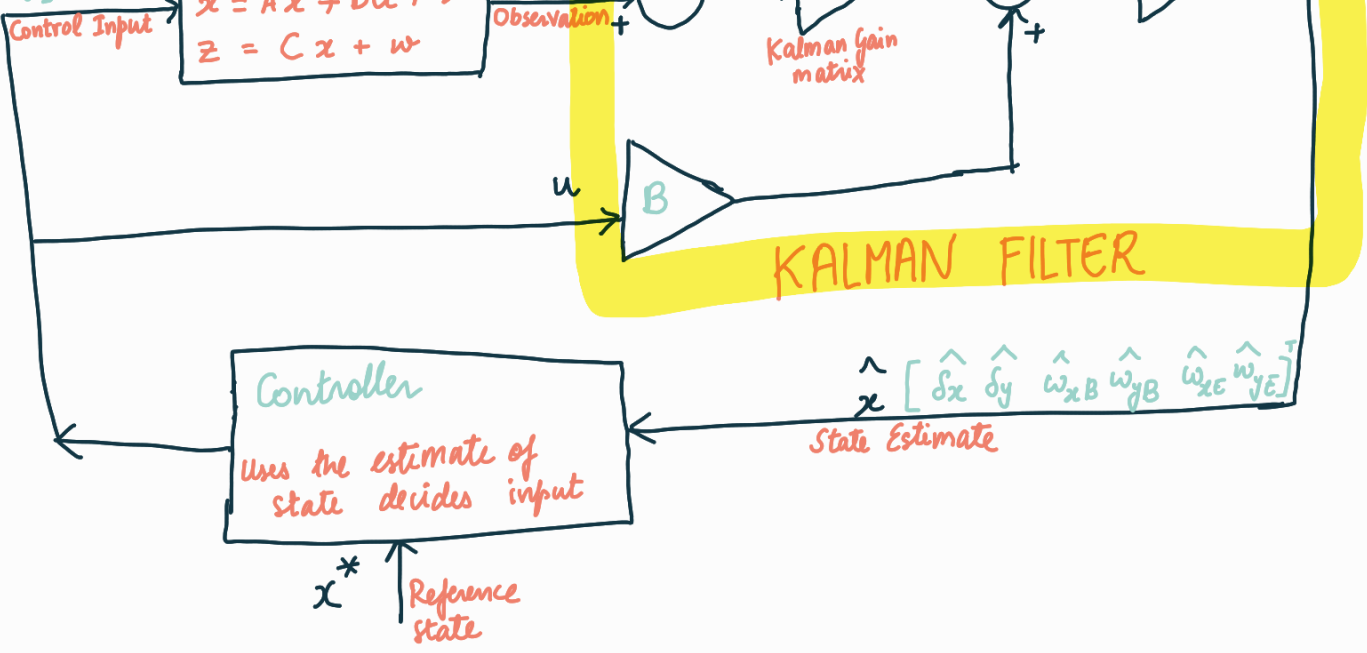
## Block Diagram



**Q1 b.**

$$\begin{bmatrix} T_x/J_d \\ T_y/J_d \end{bmatrix} u$$



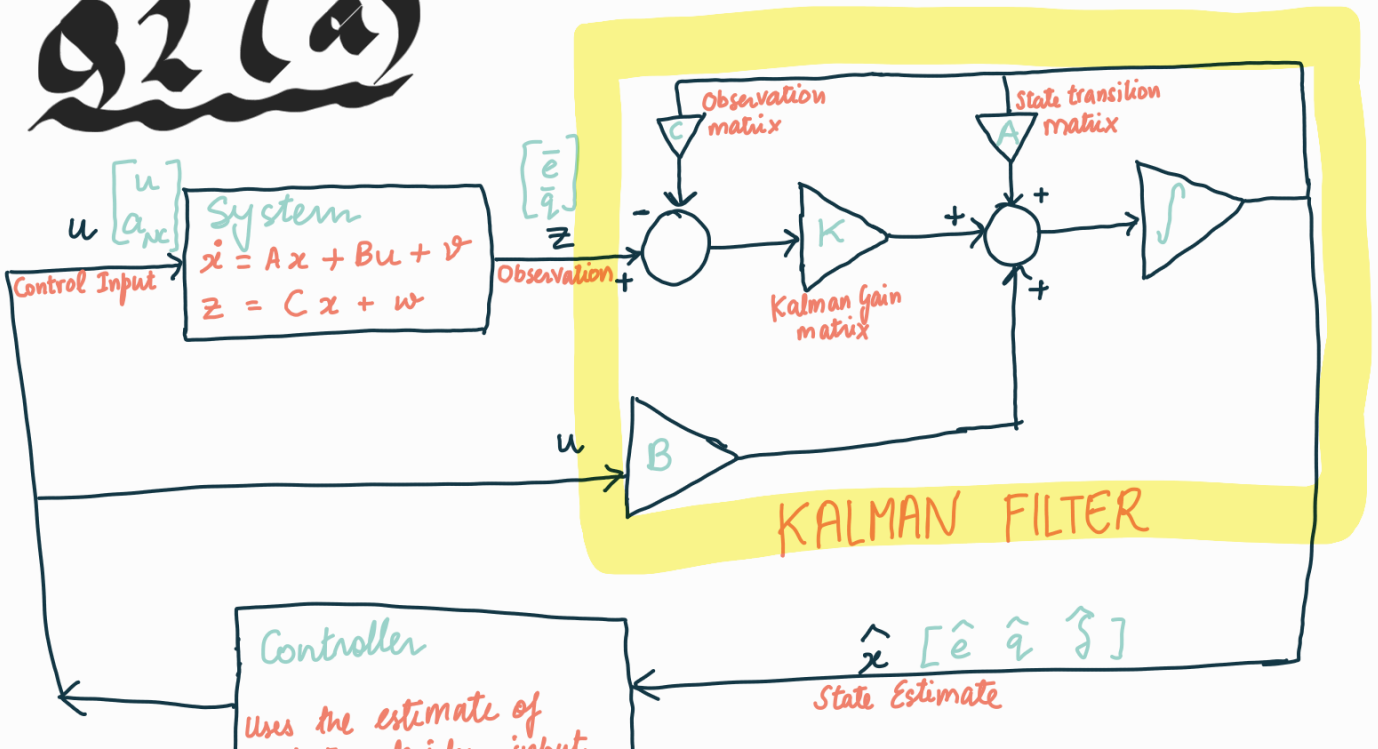


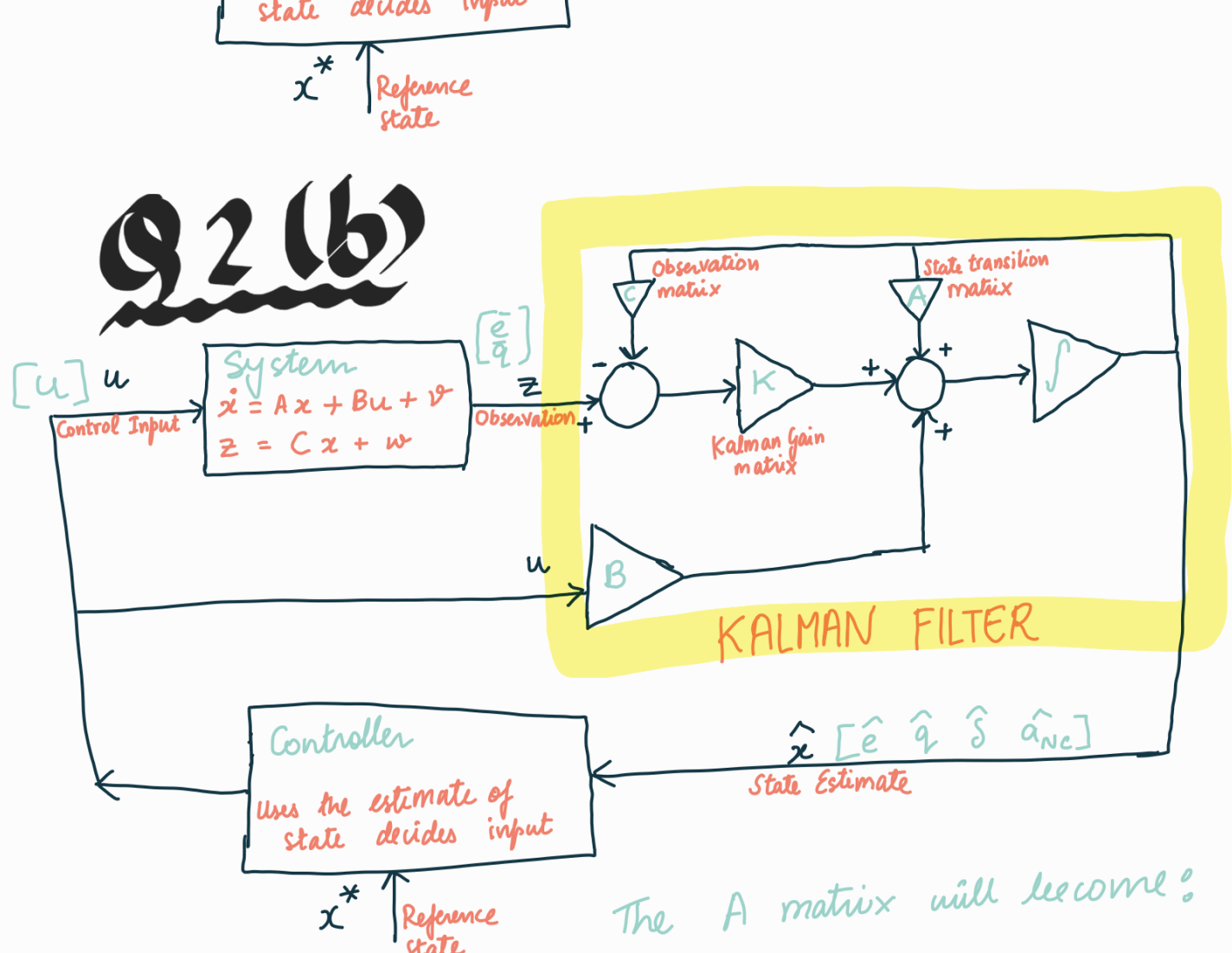
Q2 b.

In part a, there were 2 control inputs  $[u, a_{NC}]^T$  and 3 states. In this part, there will be 1 control input  $[u]$   $[e, q, \dot{s}]^T$  and 4 states  $[e, q, \dot{s}, a_{NC}]^T$ . As  $a_{NC}$  is a constant  $\ddot{a}_{NC} = 0$  and  $\dot{v}_q = 0$ .

Incorporating it into the states makes sense as the kalman estimates the states. Earlier, it was kept as an input because it was known.

Q2 (a)





The A matrix will become:

$$\begin{bmatrix} \dot{e} \\ \dot{q} \\ \dot{s} \\ \dot{a}_{NC} \end{bmatrix} = \begin{bmatrix} z_{\alpha}/\nu & -z_{\alpha} & \frac{z_s}{\nu} & -\frac{z_{\alpha}}{\nu} \\ -\frac{M\alpha}{z_{\alpha}} & Mq & \left(Mg - \frac{M\alpha}{z_{\alpha}}z_s\right) & \frac{M\alpha}{z_{\alpha}} \\ 0 & 0 & -1/\nu & 0 \\ 0 & 0 & 0 & 0 \end{bmatrix} \begin{bmatrix} e \\ q \\ s \\ a_{NC} \end{bmatrix}$$

$$+ \begin{bmatrix} -z_s/\nu \\ 0 \\ 1/\nu \\ 0 \end{bmatrix} [u]$$

Fence we get Q as :

$$V \cdot \begin{bmatrix} (z_s/\nu)^2 & 0 & -z_s/\nu^2 & 0 \\ 0 & 0 & 0 & 0 \\ -z_s/\nu^2 & 0 & 1/\nu^2 & 0 \\ 0 & 0 & 0 & 0 \end{bmatrix}$$

$$\begin{bmatrix} \bar{e} \\ \bar{q} \end{bmatrix} = \begin{bmatrix} 1 & 0 & 0 & 0 \\ 0 & 1 & 0 & 0 \end{bmatrix} \begin{bmatrix} e \\ q \\ s \\ a_{NC} \end{bmatrix} + \begin{bmatrix} w_1 \\ w_2 \end{bmatrix}$$

$\overset{C}{\curvearrowleft}$

$$\begin{bmatrix} S \\ a_{NC} \end{bmatrix} \quad \left( \text{Hence we get } R \text{ as:} \right) \quad \begin{bmatrix} w_A & 0 \\ 0 & w_B \end{bmatrix}$$

# Discretization

We have the continuous time system as:

$$\dot{x} = Ax + Bu + w \quad \begin{array}{l} \text{Process noise} \\ \text{Covariance} = Q'(t)^2 \end{array}$$

$$z = Cx + v \quad \begin{array}{l} \text{Measurement Noise} \\ \text{Covariance} = R'(t)^2 \end{array}$$

The solution for such a system is :-

$$x(t) = e^{At}x(0) + \int_0^t e^{A(t-\tau)}(Bu(\tau) + w(\tau)) d\tau$$

For a small  $t = h$ , we can write it as: (with  $x(0) = x_{n-1}$ ,  $x(h) = x_n$ )

$$x_n = e^{Ah}x_{n-1} + \left( \int_0^h e^{A\tau} d\tau \right) \cdot (Bu_n + w_n)$$

{we assume  $u(\tau) = u_n$  (constant) and  $w(\tau) = w_n$  (constant) with covariance as defined by  $\tau \in (0, h)$  the covariance of  $w(t)$ }

$$\int_0^h e^{A\tau} d\tau = \int_0^h \left( I + A\tau + \frac{A^2\tau^2}{2!} + \frac{A^3\tau^3}{3!} + \dots \right) d\tau$$

$$= \left( h + \frac{Ah^2}{2!} + \frac{A^2h^3}{3!} + \dots \right) = E$$

we numerically compute this matrix. = E

Hence we get the form:

$$x_n = F x_{n-1} + G u_n + w_n$$

$\left\{ \begin{array}{l} G = E B' \\ \text{with noise } \Theta_n^{\text{cov}} = E \left( \int_0^h Q(t) dt \right) E^T \end{array} \right\}$

$$z_n = H_n x_n + v_n$$

$\left\{ \text{Discretized noise} \right\}$

# Finding Equilibrium Point

$$\dot{e} = \frac{Z_\alpha}{V} e - Z_\alpha q + \frac{Z_\delta}{\tau} \delta - \frac{Z_\delta}{\tau} u - \frac{Z_\alpha}{V} a_{NC}$$

$$\dot{q} = -\frac{M_\alpha}{Z_\alpha} e + M_q q + \left( M_\delta - \frac{M_\alpha}{Z_\alpha} Z_\delta \right) \delta + \frac{M_\alpha}{Z_\alpha} a_{NC}$$

$$\dot{\delta} = -\frac{1}{\tau} \delta + \frac{1}{\tau} u$$

For eq. point, we want  $e = 0$   $\{ a_N = a_{NC} \}$   
 $\{ a_{NC} \neq 0 \}$   $\dot{e} = 0$   $\{ \text{error doesn't become non-zero} \}$   
 $\dot{q}, \dot{\delta} = 0$   $\{ \text{steady state} \}$

$$\cancel{\dot{e} = \frac{Z_\alpha}{V} e - Z_\alpha q + \left( \frac{Z_\delta}{\tau} \delta - \frac{Z_\delta}{\tau} u \right) - \frac{Z_\alpha}{V} a_{NC}}$$

$$\cancel{\dot{q} = -\frac{M_\alpha}{Z_\alpha} e + M_q q + \left( M_\delta - \frac{M_\alpha}{Z_\alpha} Z_\delta \right) \delta + \frac{M_\alpha}{Z_\alpha} a_{NC}}$$

$$\cancel{\dot{\delta} = -\frac{1}{\tau} \delta + \frac{1}{\tau} u} \Rightarrow u = \delta$$

Hence get:  $\delta = u$

$$z_K q + \frac{z_\alpha}{V} a_{NC} = 0 \Rightarrow q = -\frac{a_{NC}}{V}$$

$$\delta = \frac{\frac{M_\alpha}{z_\alpha} a_{NC}}{\frac{M_\alpha}{z_\alpha} z_\delta - M_\delta} \Rightarrow \delta = \frac{\frac{M_\alpha}{z_\alpha} a_{NC}}{z_\delta \cdot M_\alpha - M_\delta z_\alpha} a_{NC}$$

Equilibrium point :=  $\begin{bmatrix} e_0 \\ q_0 \\ \delta_0 \end{bmatrix} = \begin{bmatrix} 0 \\ -\frac{a_{NC}}{V} \\ \frac{M_\alpha}{z_\delta \cdot M_\alpha - M_\delta z_\alpha} a_{NC} \end{bmatrix}$  &  $u_0 = \frac{M_\alpha}{z_\delta \cdot M_\alpha - M_\delta z_\alpha} a_{NC}$

Hence if we define:  $\Delta q = q - q_0 = q + \frac{a_{NC}}{V}$  |  $\Delta u = u - u_0$   
 $\Delta \delta = \delta - \delta_0$  |

Hence, for a fixed  $a_{NC}$ :  $\begin{bmatrix} \dot{e} \\ \dot{q} \\ \dot{\delta} \end{bmatrix} = \begin{bmatrix} z_\alpha/V & -z_\alpha & z_\delta/\tau \\ -M_\alpha/z_\alpha & 0 & M_\delta - M_\alpha z_\delta/z_\alpha \\ 0 & 0 & -1/\tau \end{bmatrix} \begin{bmatrix} e \\ \Delta q \\ \Delta \delta \end{bmatrix}$

$+ \begin{bmatrix} -z_\delta/\tau \\ 0 \\ 1/\tau \end{bmatrix} \Delta u$

# Q1 : Two-axis Gyro - Steady State Analysis

## Initialization

```
A = 6x6
    0      0      1      0      -1      0
    0      0      0      1      0      -1
   -30     -60     0     3000      0      0
    60     -30    -3000      0      0      0
    0      0      0      0      0      0
    0      0      0      0      0      0

B = 6x2
    0      0
    0      0
    1      0
    0      1
    0      0
    0      0

C = 2x6
    1      0      0      0      0      0
    0      1      0      0      0      0

Q = 6x6
    0      0      0      0      0      0
    0      0      0      0      0      0
    0      0      0      0      0      0
    0      0      0      0      0      0
    0      0      0      0      1      0
    0      0      0      0      0      1

R = 2x2
    1      0
    0      1
```

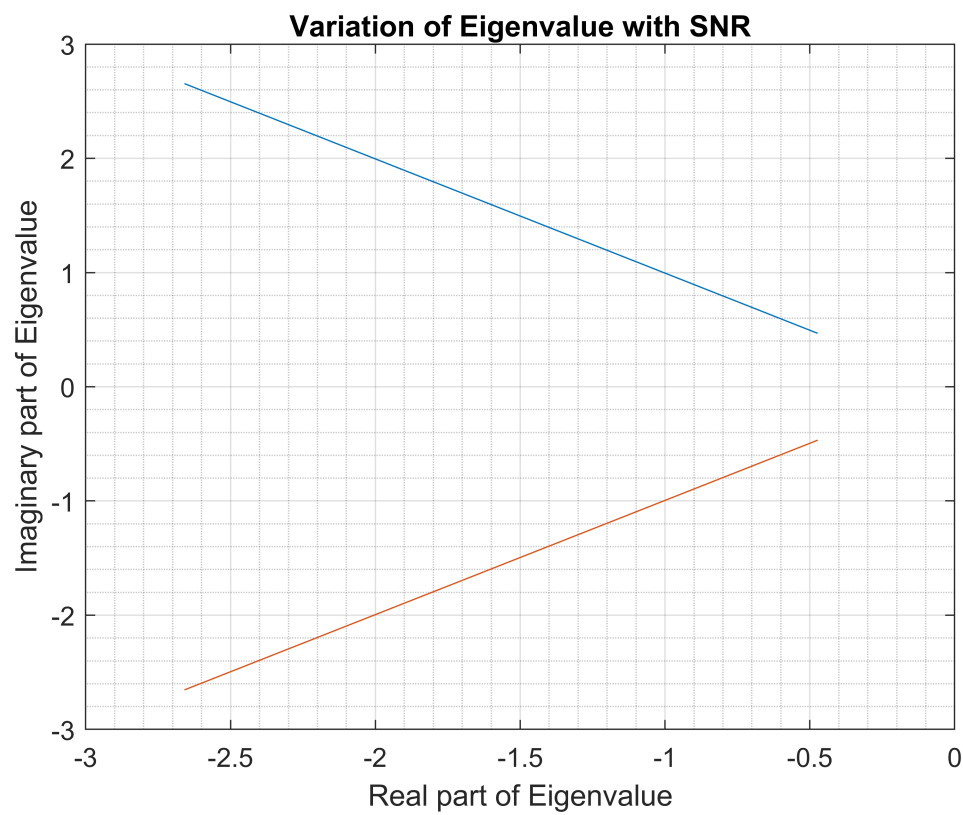
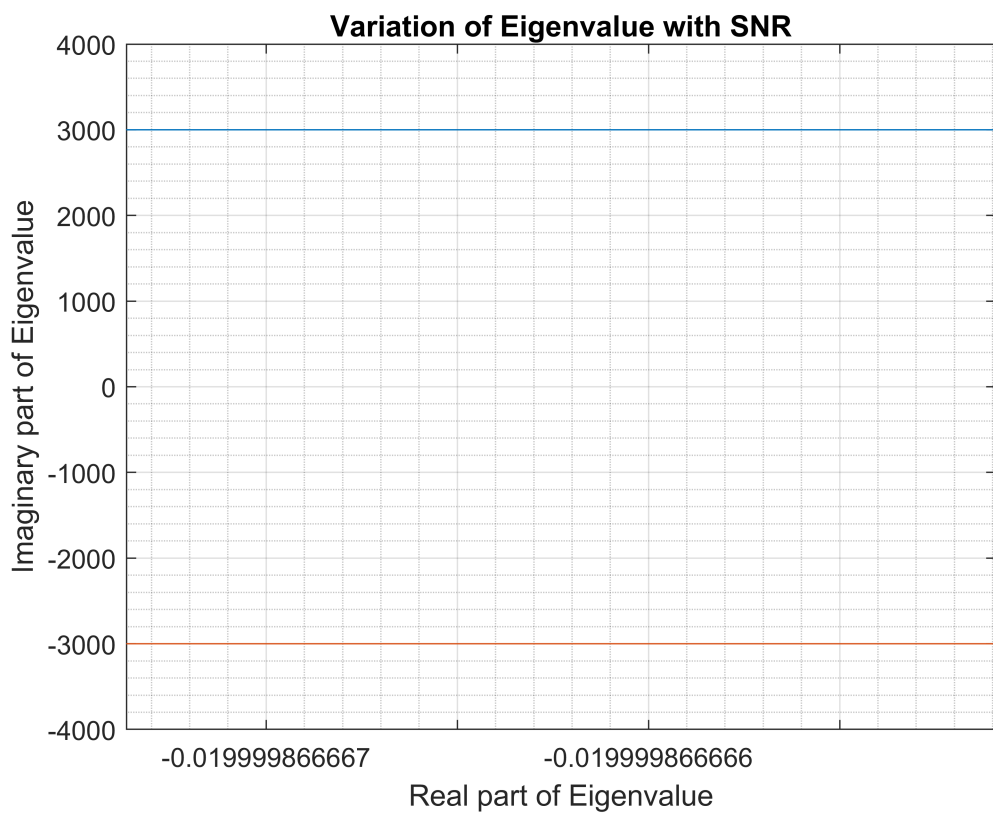
Matrices are initialized appropriately and the Q and R matrices will be scaled for different values of Signal-to-Noise Ratio

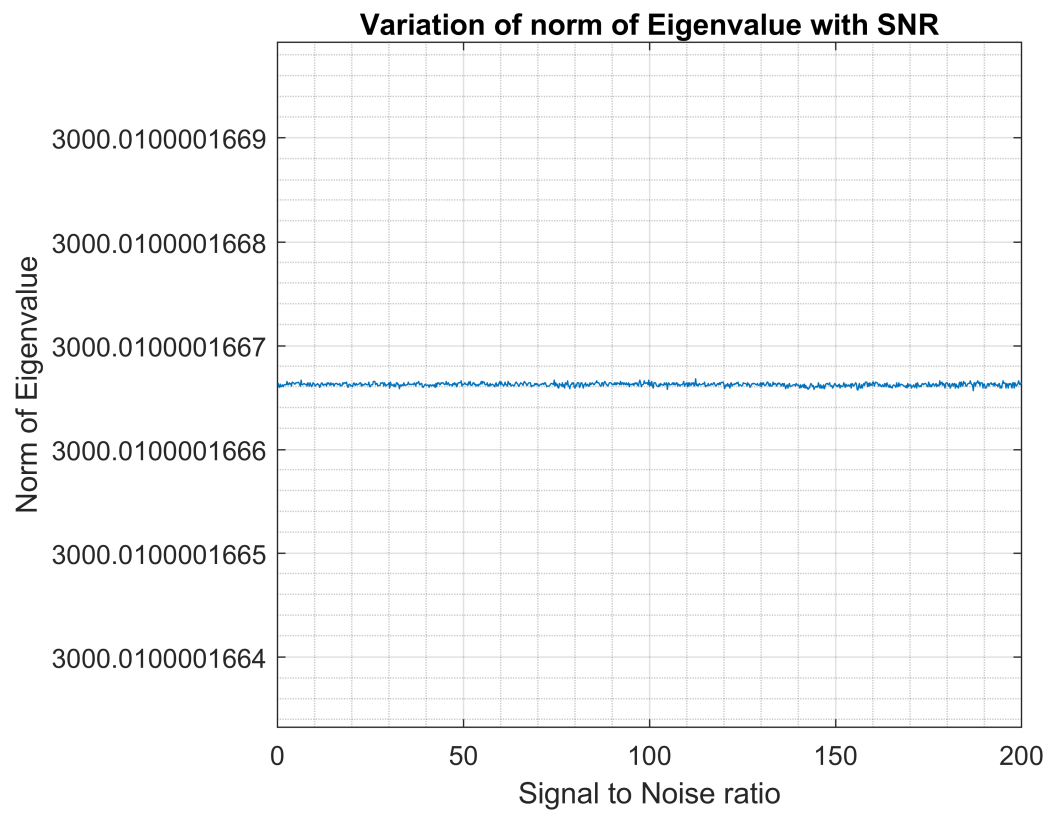
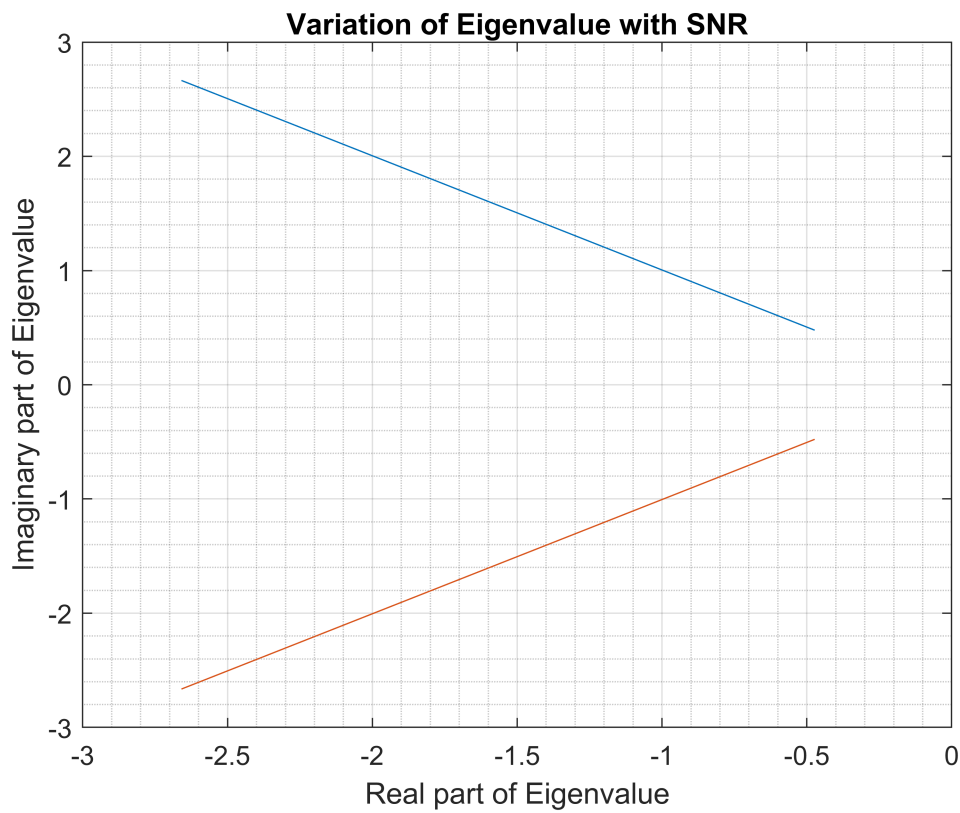
## Computation of Gain elements and Closed Loop Poles

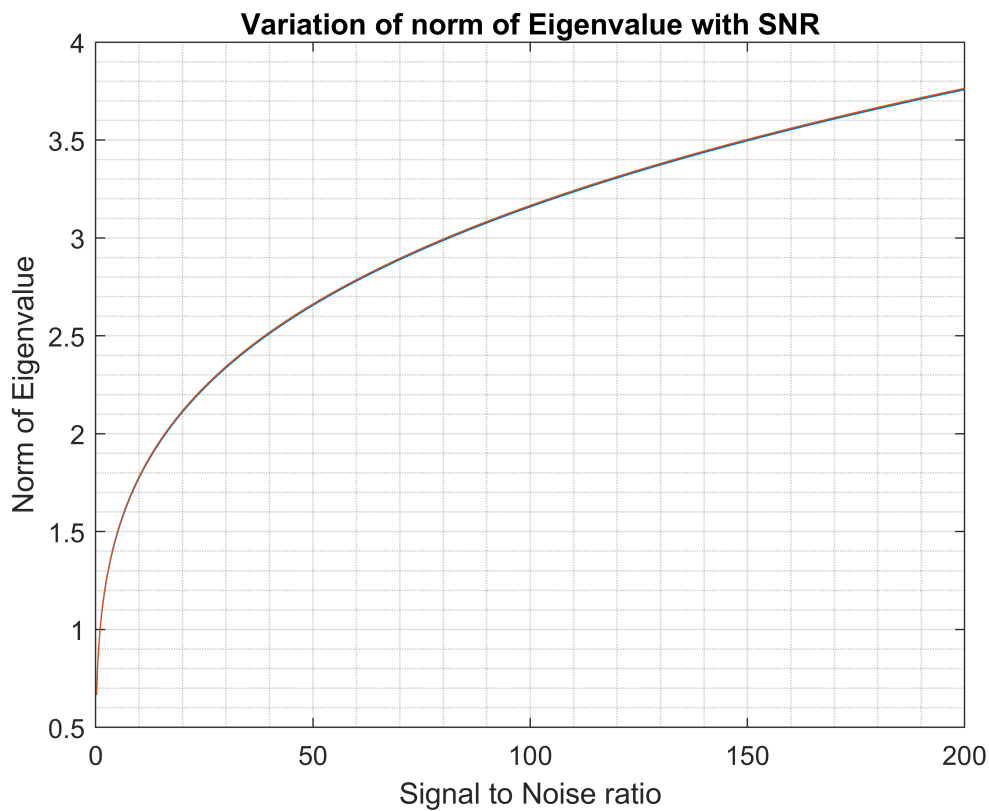
```
arr_noise = 1x1000
 0.2000    0.4000    0.6000    0.8000    1.0000    1.2000    1.4000    1.6000 ...
N = 1000
```

Array of Signal-to-Noise Ratio is initialized and the Gain elements are calculated using the LQR dual problem.

## Plotting Closed Loop Poles

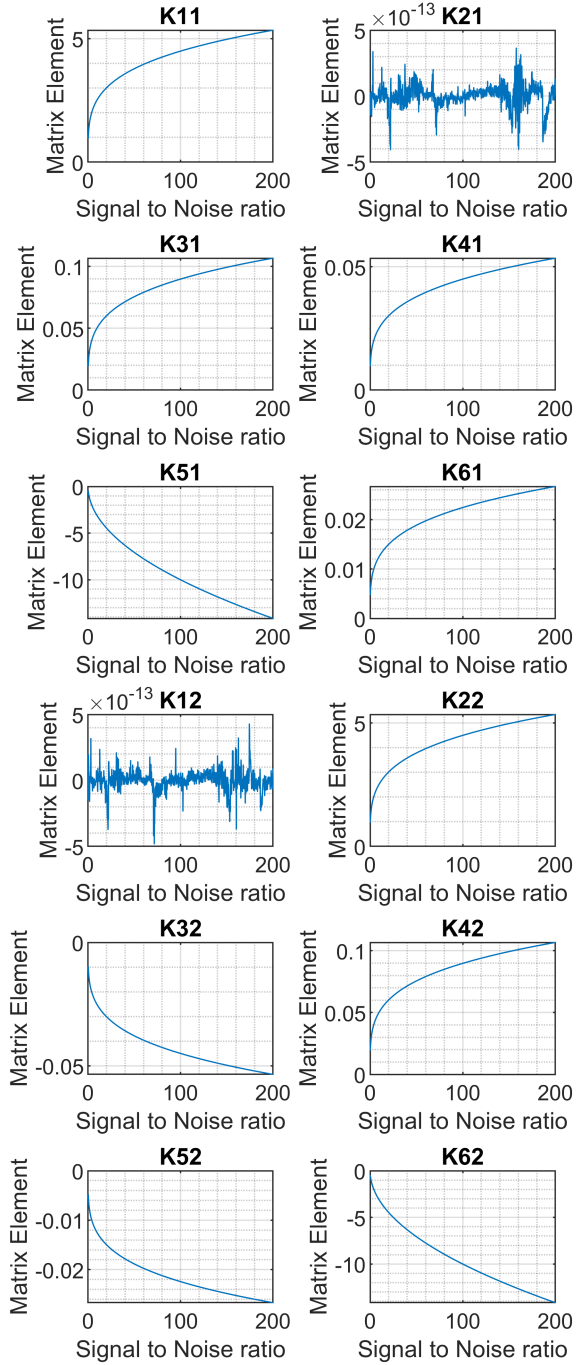






We observe that the closed loop poles have a larger negative real part, and hence the observer will converge to the state values sooner when the SNR is higher. It makes sense, as for smaller noise, we expect faster convergence. There three complex conjugate eigenvalue pairs, of which are two doubly repeated eigenvalues .

### Plotting Kalman Gain matrix



We observe that each element of the gain matrix is going away from 0 with increasing SNR, i.e., we are giving more weightage to measurement. This makes sense as when the measurement noise is lesser, the preference should be given to measurement. When the measurement noise is lesser, it makes sense to give more weightage to the prediction which corresponds to a smaller value of K.

## Q2 : Missile Autopilot - Steady State Analysis

### Initialization

```
A = 3x3
105 x
-0.0000    0.0417   -1.1150
-0.0000        0    -0.0060
     0        0    -0.0010

B = 3x2
105 x
  1.1150    0.0000
     0      0.0000
  0.0010        0

C = 2x3
  1      0      0
     0      1      0

Q = 3x3
1010 x
  1.2432      0    0.0011
     0      0      0
  0.0011      0    0.0000
```

Matrices are initialized appropriately and the Q and R matrices will be scaled for different values of Signal-to-Noise Ratio.

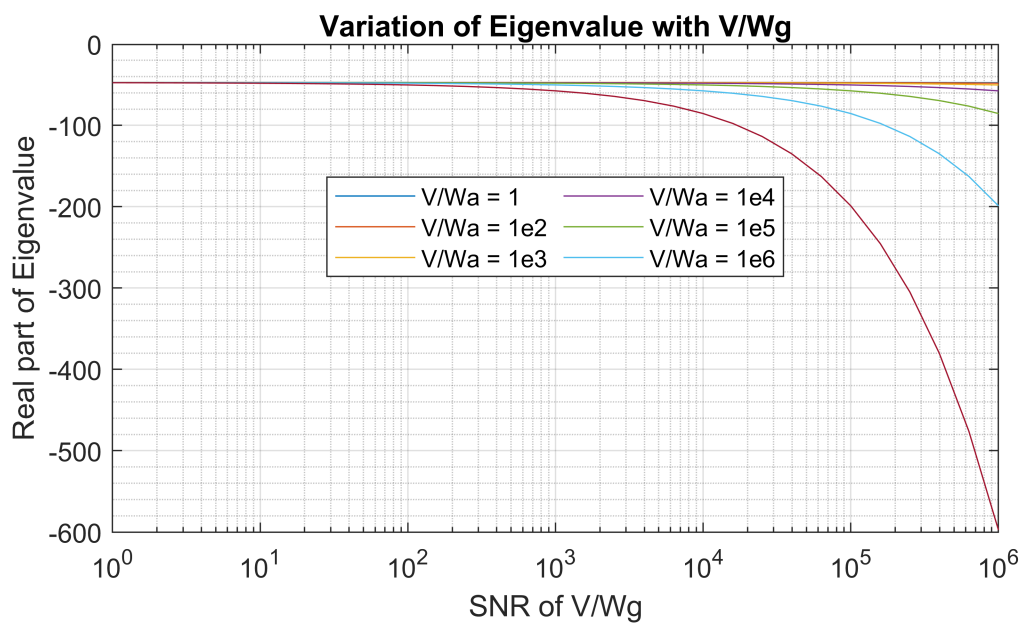
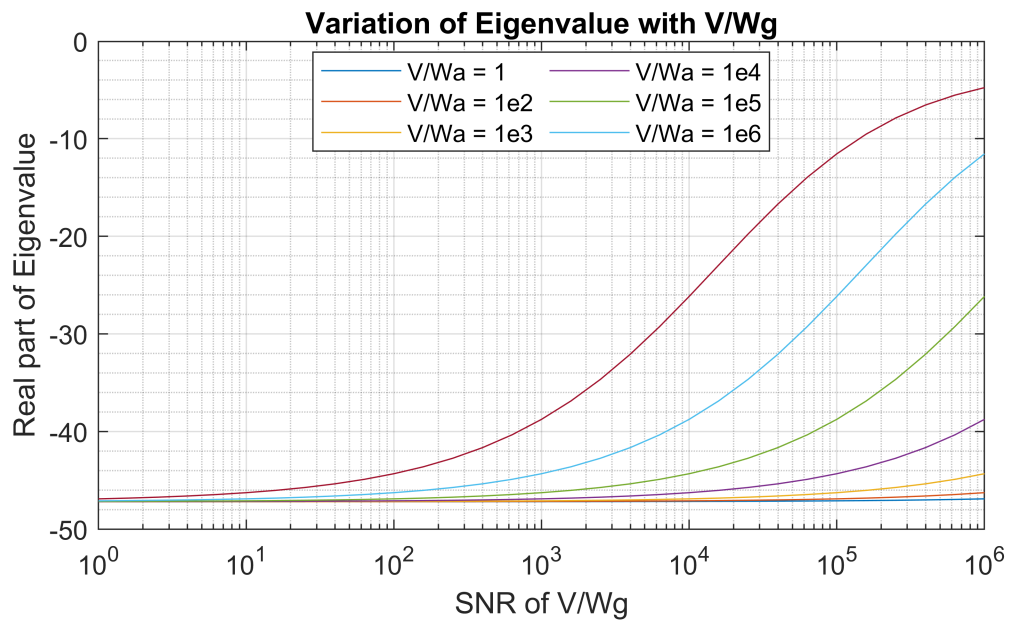
### Computation

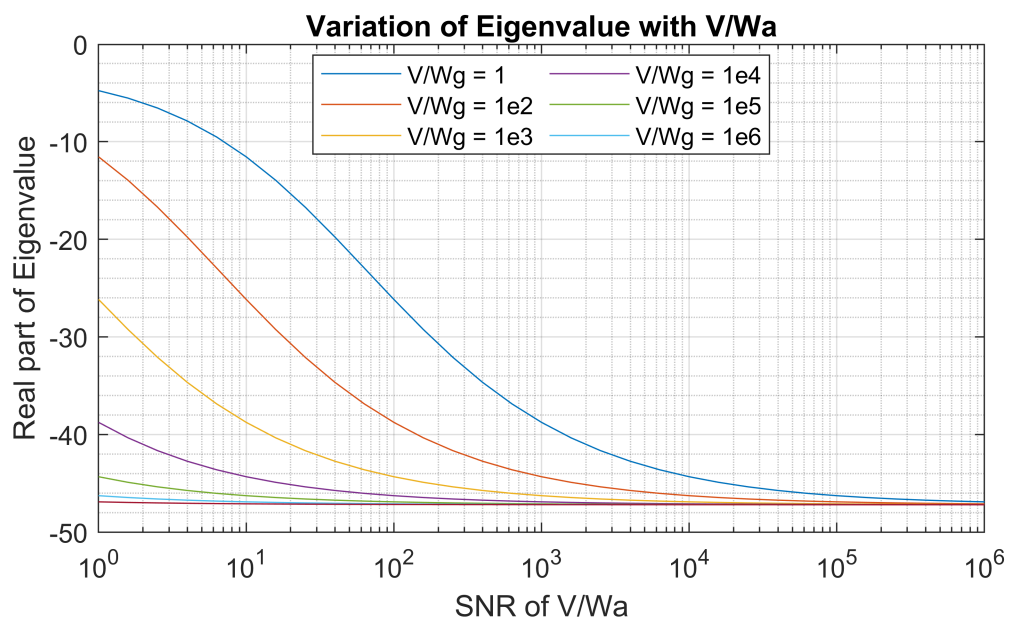
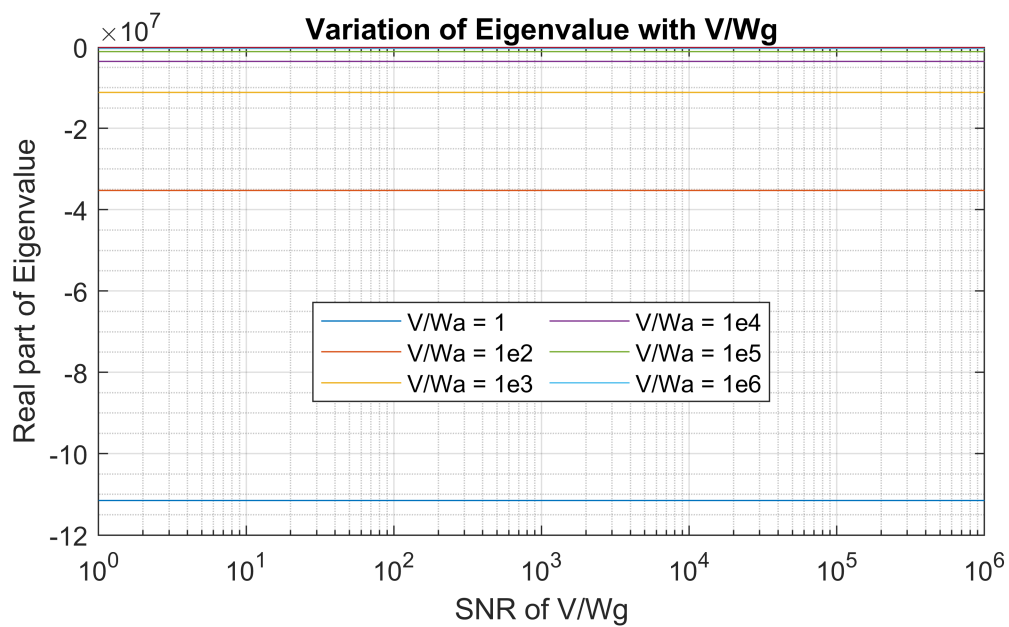
```
N = 31
```

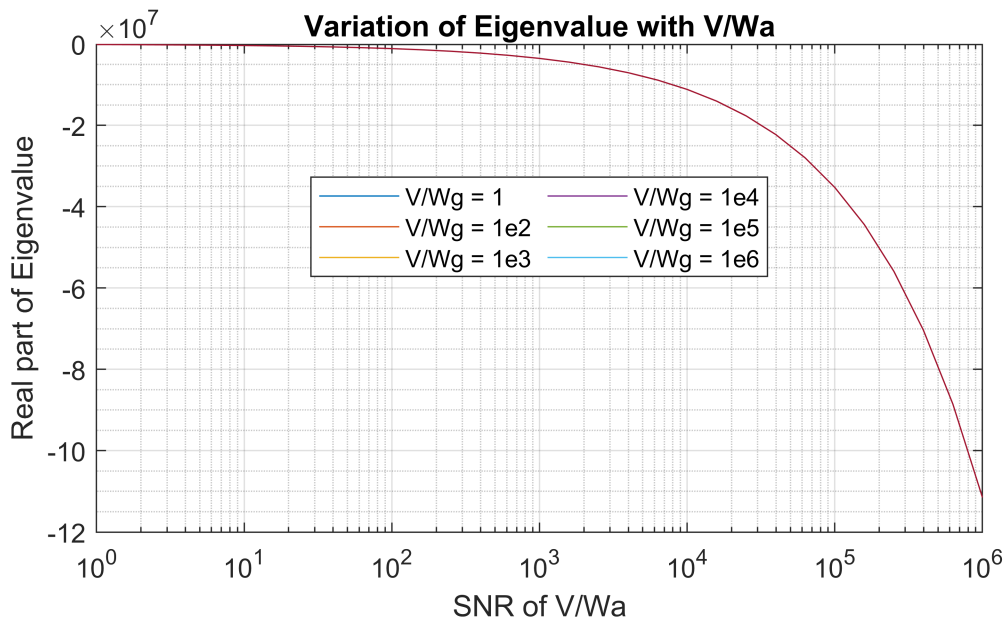
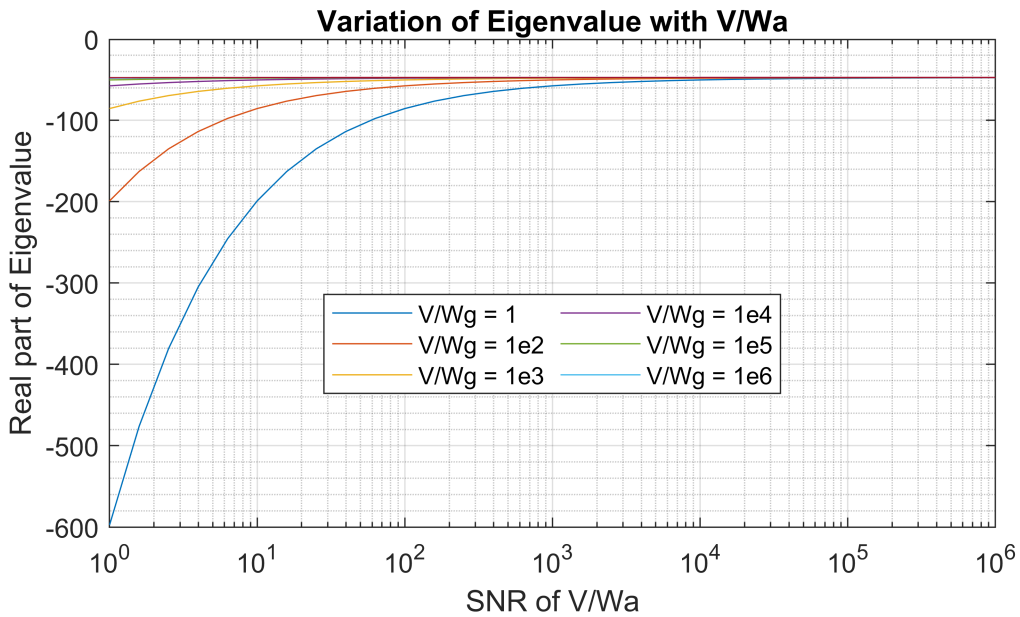
Array of Signal-to-Noise Ratio is initialized and the Gain elements are calculated using the LQR dual problem.

### Closed Loop Poles

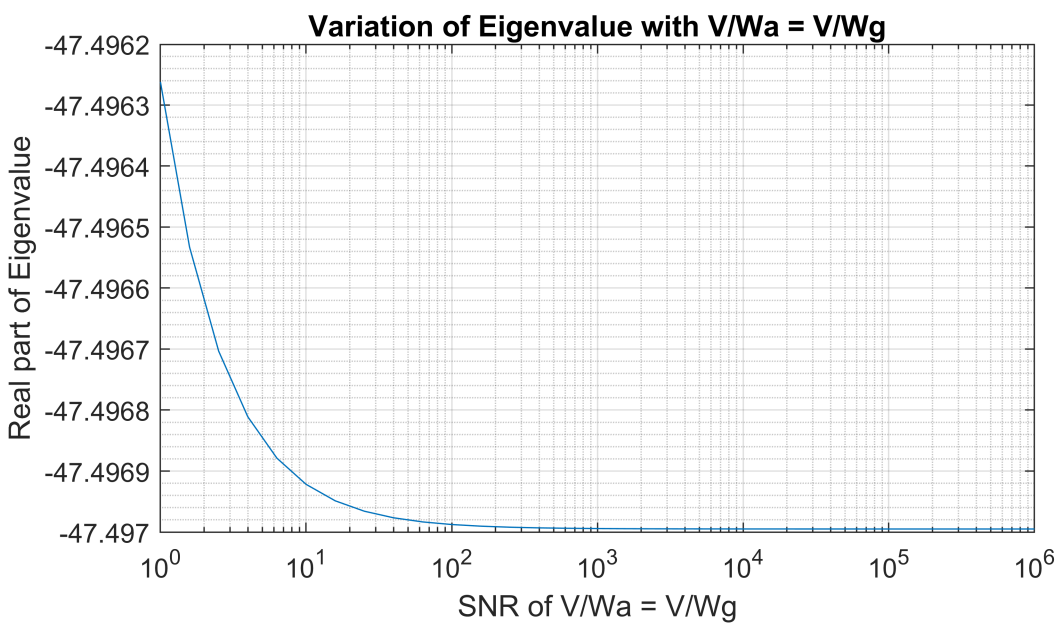
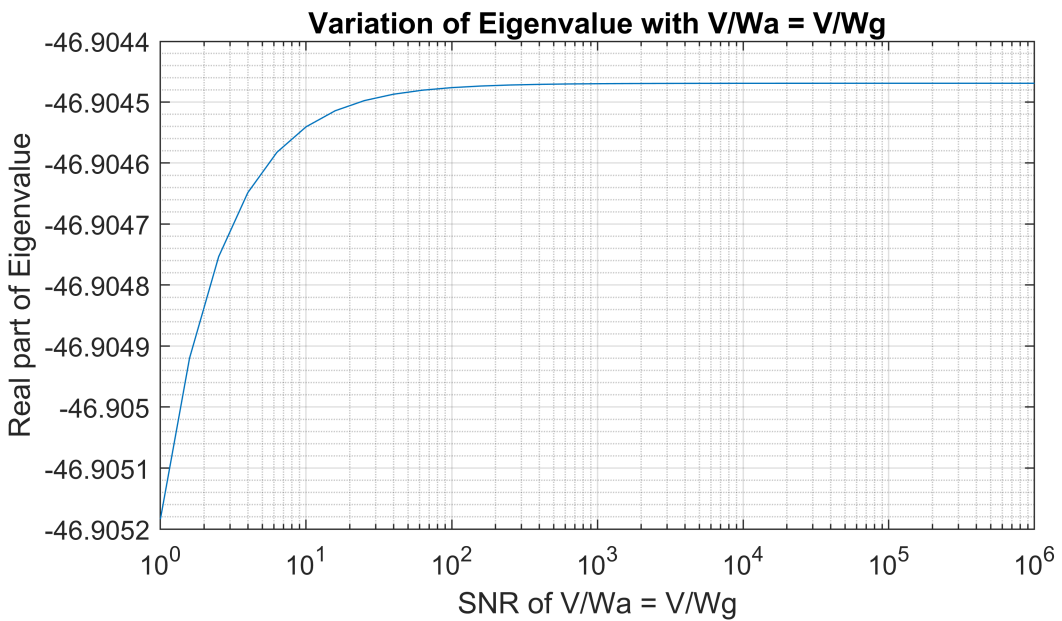
We observe that eigenvalues are always real.

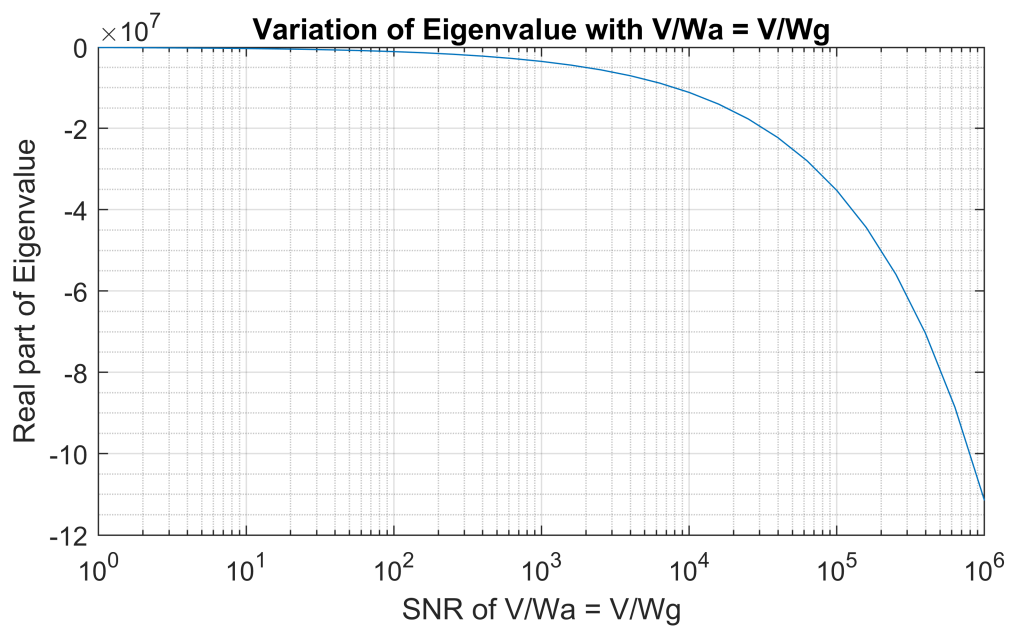






When we are varying only one of the noise element ( $W_a$  or  $W_g$ ), we observe that some eigenvalues get more negative, while other get more positive. It corresponds to the fact that some estimated states will reach the true value faster than the others.

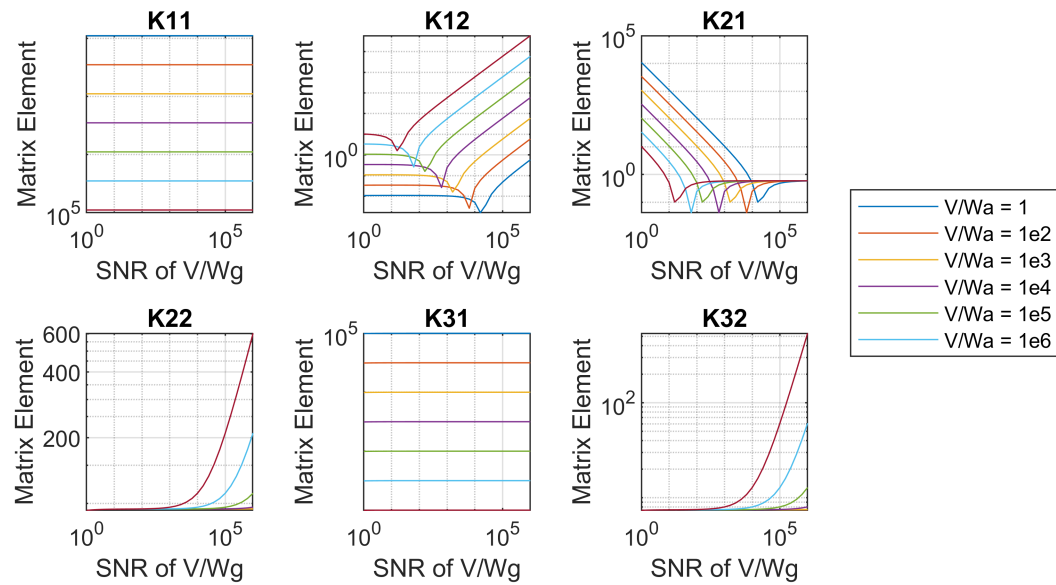




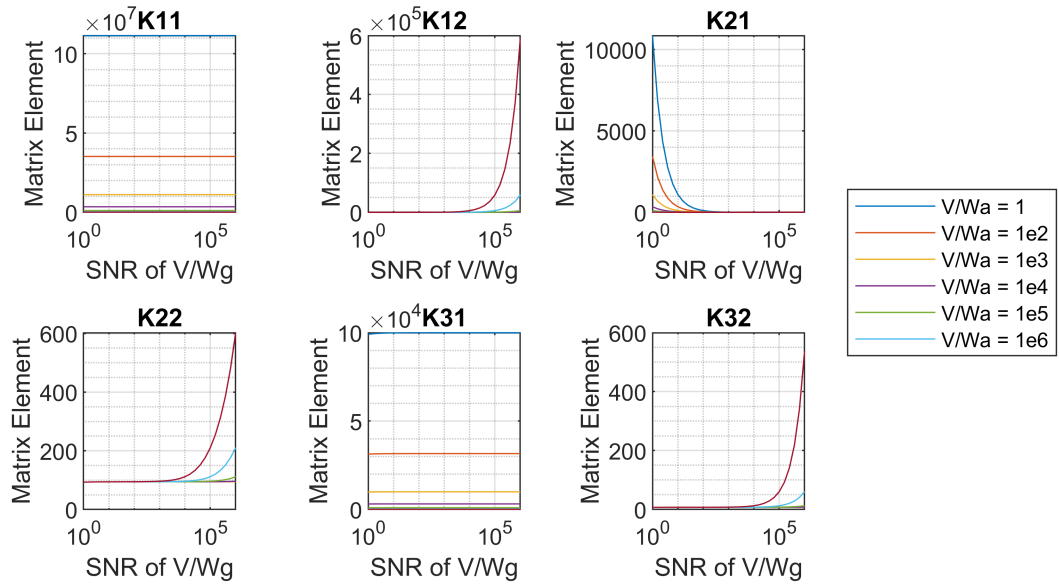
When we vary both  $W_a$  and  $W_g$ , we observe that two eigenvalues don't change much, but the third decreases a lot, hence the filter converges faster..

## Kalman Gain Matrix

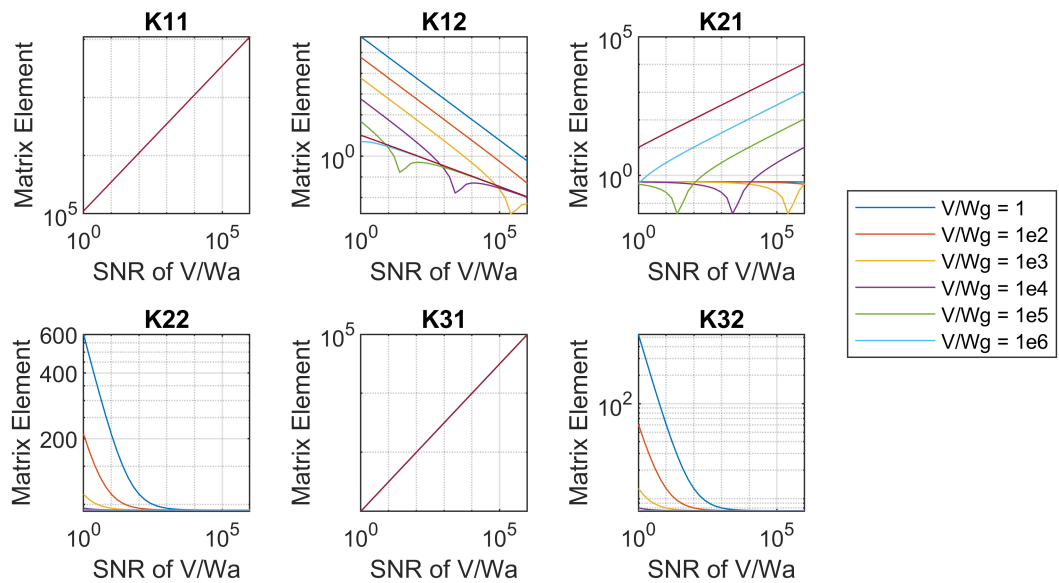
Log-Log(mod) plot of variation of the Gain Elements with  $V/W_g$



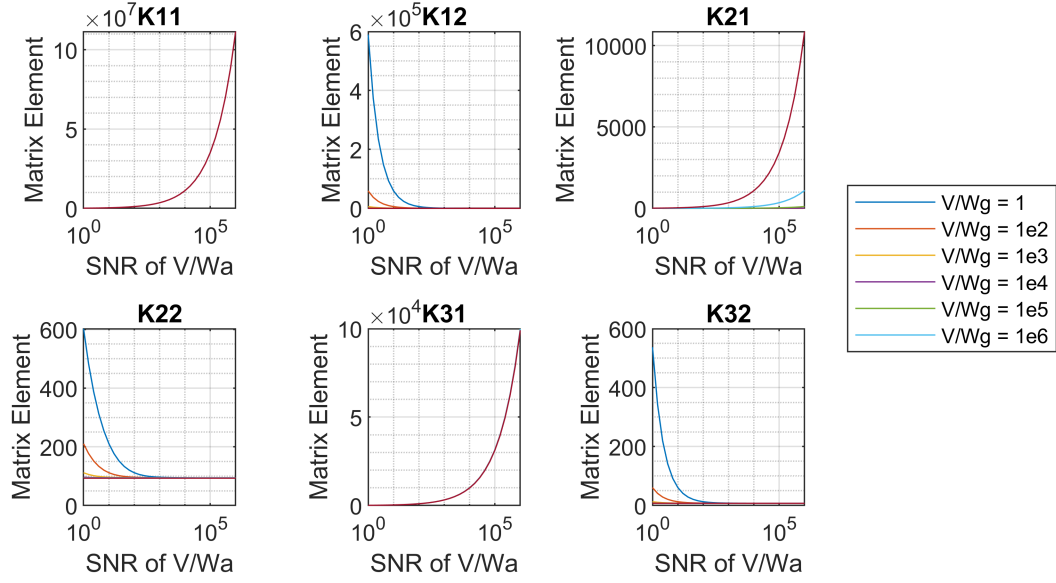
Semi-Log (x) plot of variation of the Gain Elements with  $V/W_g$



Log-Log(mod) plot of variation of the Gain Elements with  $V/Wa$



Semi-Log (x) plot of variation of the Gain Elements with  $V/Wa$



We see a kink in the graphs, it corresponds to the element changing sign. The value  $K_{11}$  does not vary with variation of  $V/W_g$ .

The general trend that increment of noise leads to an increment in the corresponding gain element is observed in each of the cases. When  $W_a$  is larger, we give more weight to Gyro measurements and vice versa.

# SC651 Assignment 1: Time Evolution Analysis

Tanmay Dokania, 200070083

March 2023

## 1 Question 1: Two-Axis Gyro

### 1.1 Controller Design

Assuming we have the full state access (the Kalman observer has converged close to the true state parameters), we design a controller using the state estimate from the measurements till that instant of time.

As the control inputs  $u = [\frac{\tau_x}{J_d}, \frac{\tau_y}{J_d}]$ , control the state corresponding states of  $\omega_B$  completely, we can make it to follow  $\omega_E$  and also ensure that it drives  $\delta$  to 0. Therefore, the feedback controller will stabilize the system.

### 1.2 Simulating the System

The system has been simulated for Signal-to-Noise Ratio ranging from 0.2 to 200 in step 10, i.e., for  $SNR = [0.2, 2, 20, 200]$ .

The time variation of the estimate, measurement, and true state are shown for  $\delta_x$  and  $\delta_y$ .

The initial estimate of the state is assumed to be  $[0, 0, 0, 0, 0, 0]^T$ . However, the initial state is  $[1, 2, 1, 3, 0, 1]^T$ . As a measure of uncertainty of the initial state, the state estimate covariance matrix is taken to be:

$$P_0 = \begin{pmatrix} 1000 & 0 & 0 & 0 & 0 & 0 \\ 0 & 1000 & 0 & 0 & 0 & 0 \\ 0 & 0 & 1000 & 0 & 0 & 0 \\ 0 & 0 & 0 & 1000 & 0 & 0 \\ 0 & 0 & 0 & 0 & 1000 & 0 \\ 0 & 0 & 0 & 0 & 0 & 1000 \end{pmatrix}$$

### 1.2.1 Variation of $\delta_x$

We observe that despite large measurement noise from the sensor data, the state estimate is very close to the true state. The power of Kalman filtering algorithm is depicted clearly here.

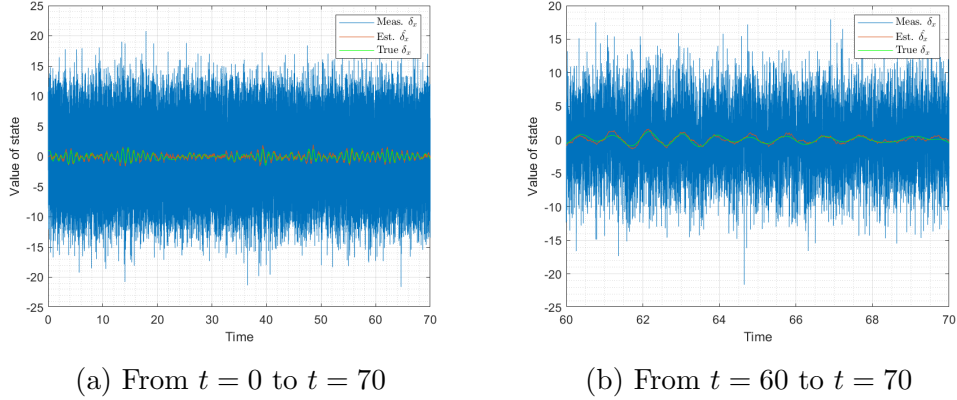


Figure 1: For Signal-to-Noise Ratio = 0.2

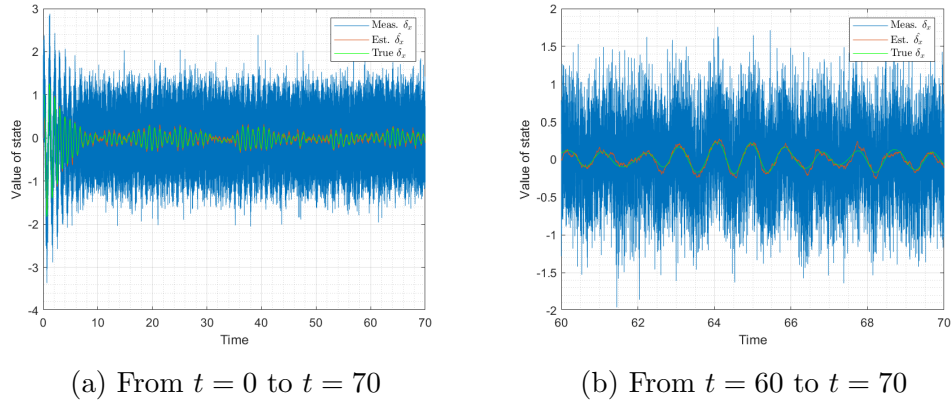


Figure 2: For Signal-to-Noise Ratio = 2

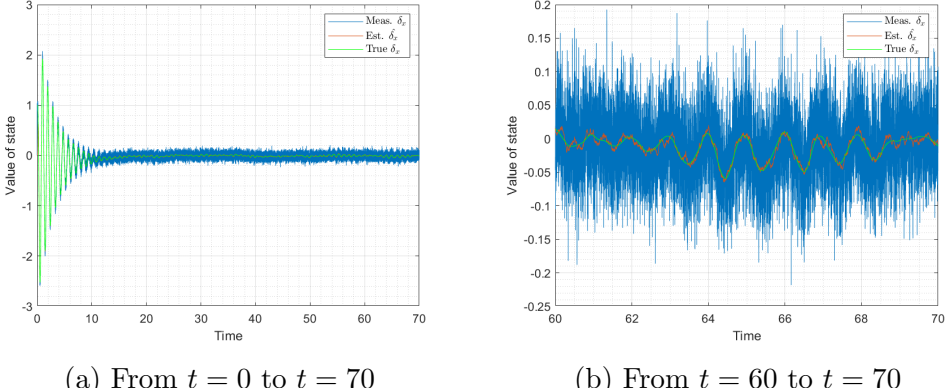


Figure 3: For Signal-to-Noise Ratio = 20

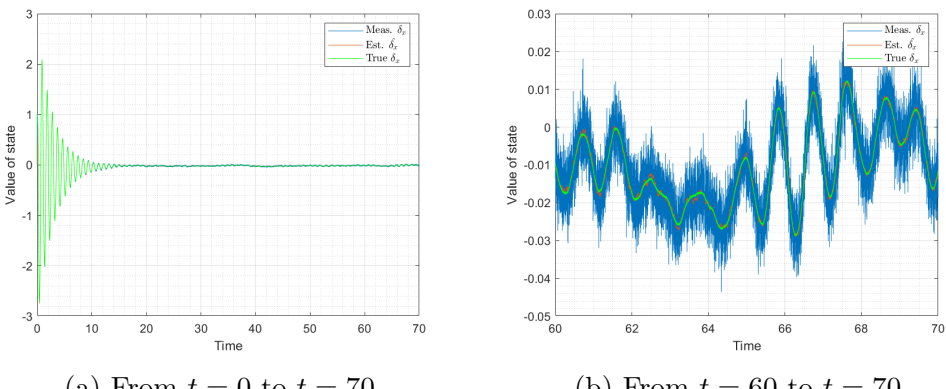
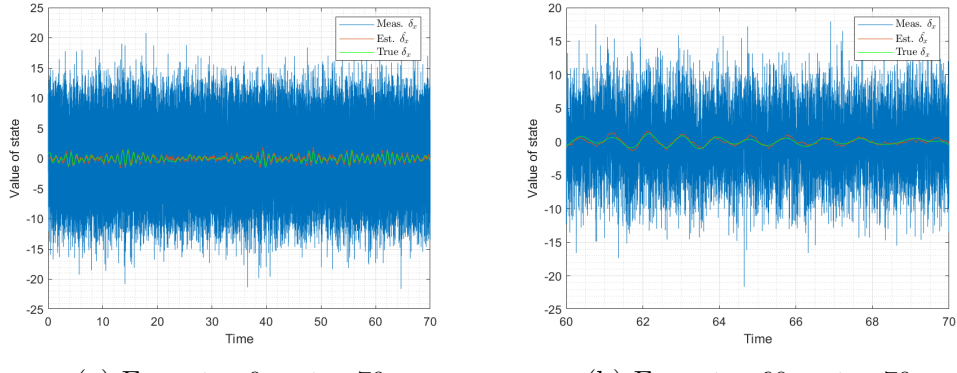


Figure 4: For Signal-to-Noise Ratio = 200

The blue line is for the measurement, and the orange line is for the estimated state, and the green line is for the true state.

### 1.2.2 Variation of $\delta_y$

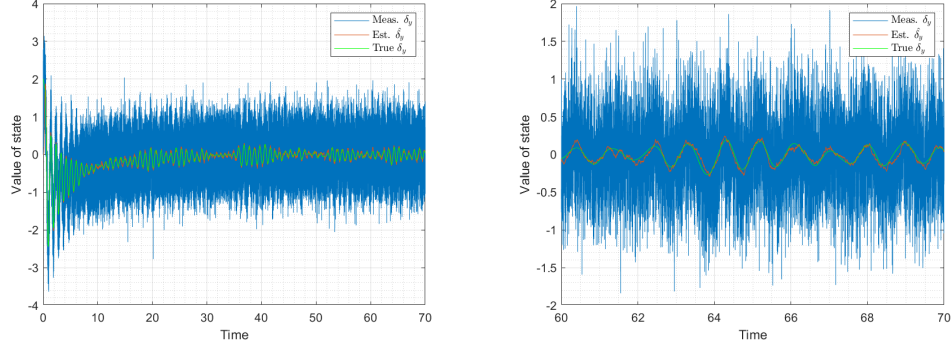
We observe that despite large measurement noise from the sensor data, the state estimate is very close to the true state. The power of Kalman filtering algorithm is depicted clearly here.



(a) From  $t = 0$  to  $t = 70$

(b) From  $t = 60$  to  $t = 70$

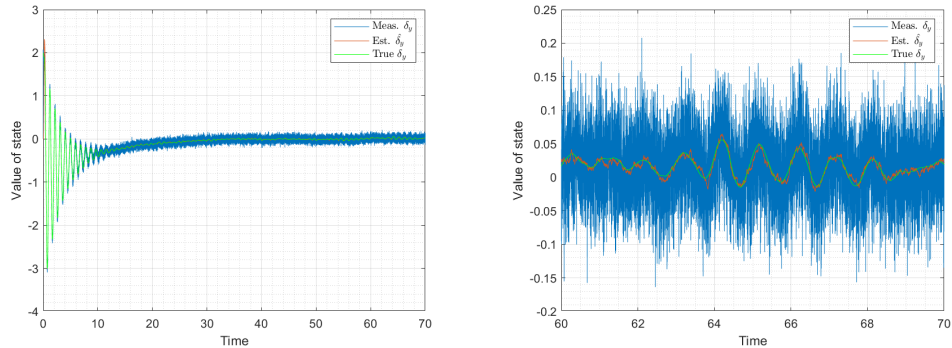
Figure 5: For Signal-to-Noise Ratio = 0.2



(a) From  $t = 0$  to  $t = 70$

(b) From  $t = 60$  to  $t = 70$

Figure 6: For Signal-to-Noise Ratio = 2



(a) From  $t = 0$  to  $t = 70$

(b) From  $t = 60$  to  $t = 70$

Figure 7: For Signal-to-Noise Ratio = 20

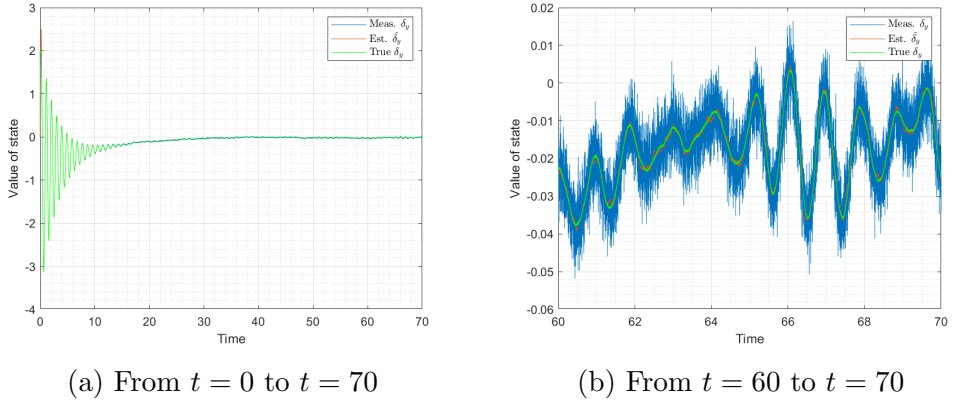


Figure 8: For Signal-to-Noise Ratio = 200

The blue line is for the measurement, the orange line is for the estimated state, and the green line is for the true state.

### 1.2.3 Variation of other states' estimate and true value

Kalman filter does a good job at estimating the other states just from the values of  $[\delta_x, \delta_y]$ . The estimate of  $[\omega_{xE}, \omega_{yE}]$  lags as the changes in that state cannot be accounted for easily. As these states change independently of the previous state. As the initial values of the states are also unknown, the states reach the correct value in the initial steps.

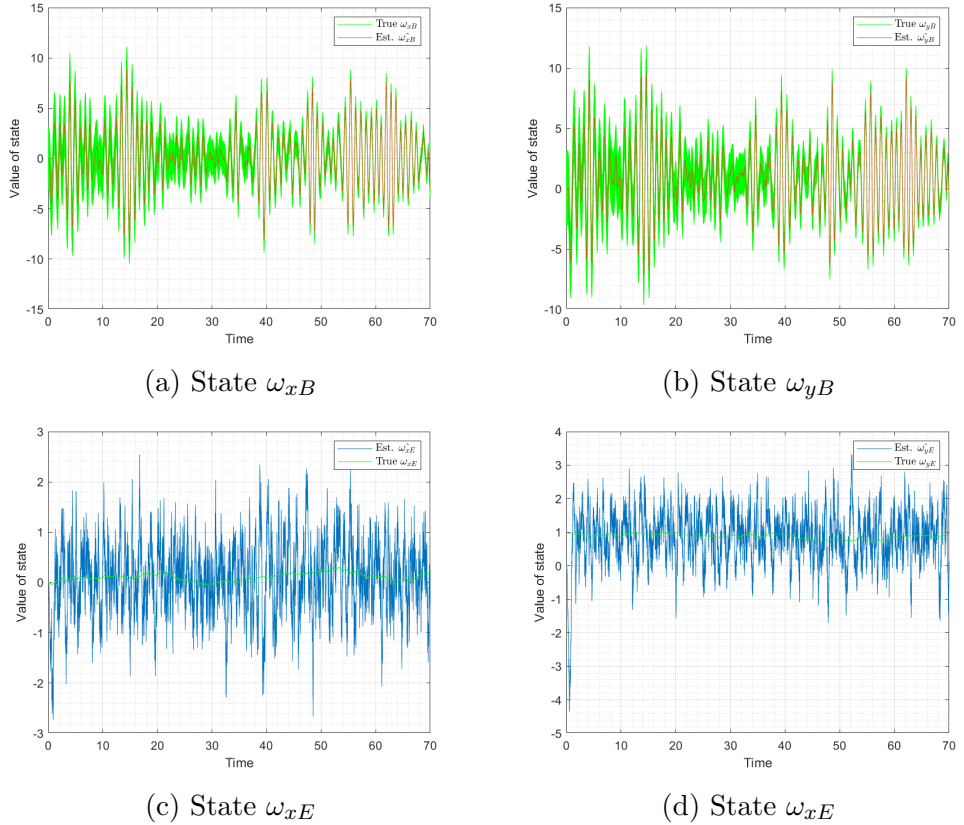


Figure 9: For Signal-to-Noise = 0.2 and time from  $t = 0$  to  $t = 70$

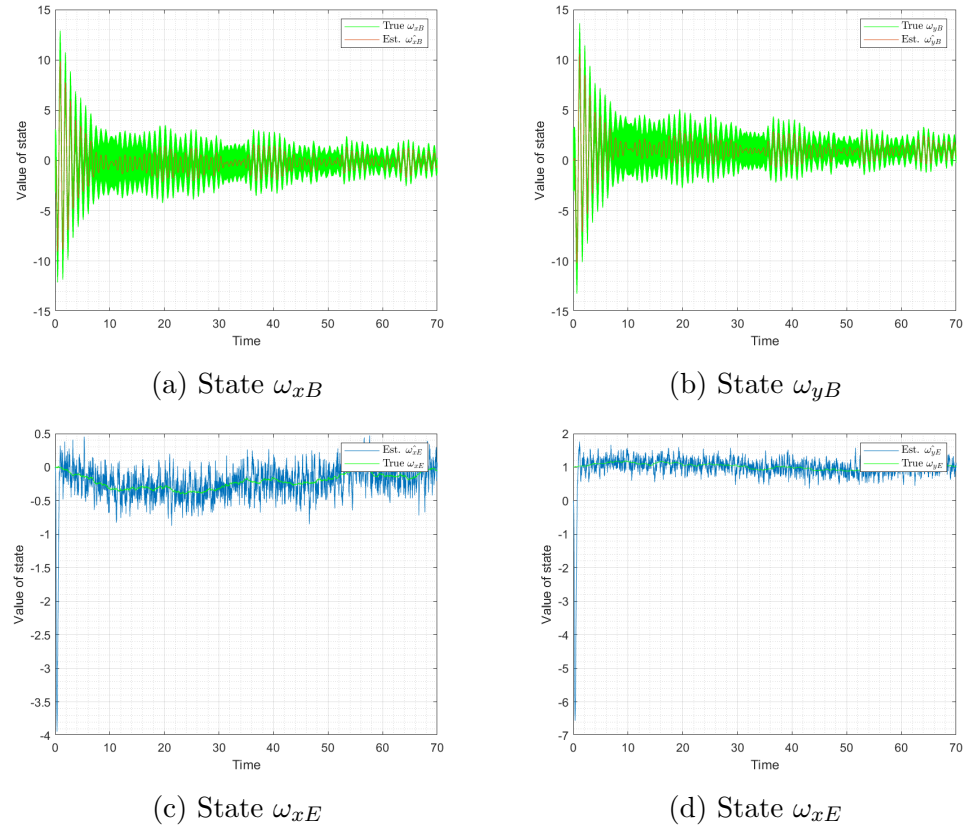


Figure 10: For Signal-to-Noise = 2 and time from  $t = 0$  to  $t = 70$

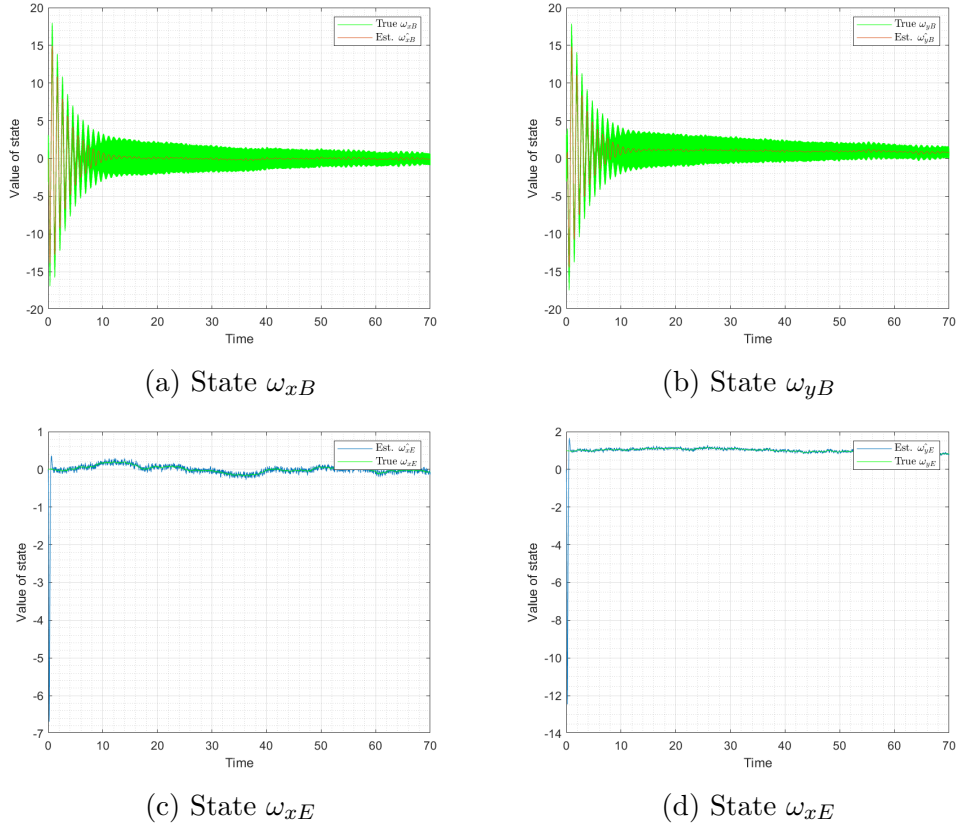


Figure 11: For Signal-to-Noise = 20 and time from  $t = 0$  to  $t = 70$

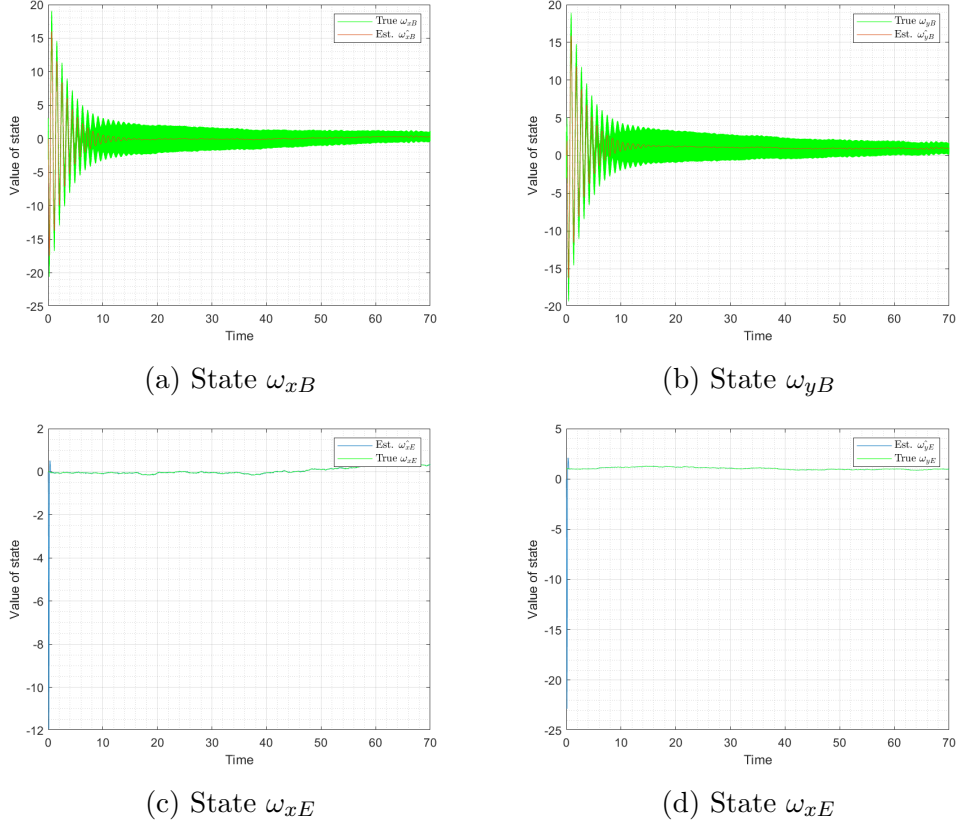


Figure 12: For Signal-to-Noise = 200 and time from  $t = 0$  to  $t = 70$

#### 1.2.4 Time evolution of the gains of the Kalman Matrix

It is observed that the gains achieve the steady state value in the initial few seconds from the start of the simulation. The plots for each of the gain element for different SNR is shown in as follows. We observe that the Kalman gains converge to the true value faster for larger values of SNR. This can be also confirmed from the fact that norm of eigenvalues of the closed loop observer were increasing for larger SNR. The plots are with same time scale.

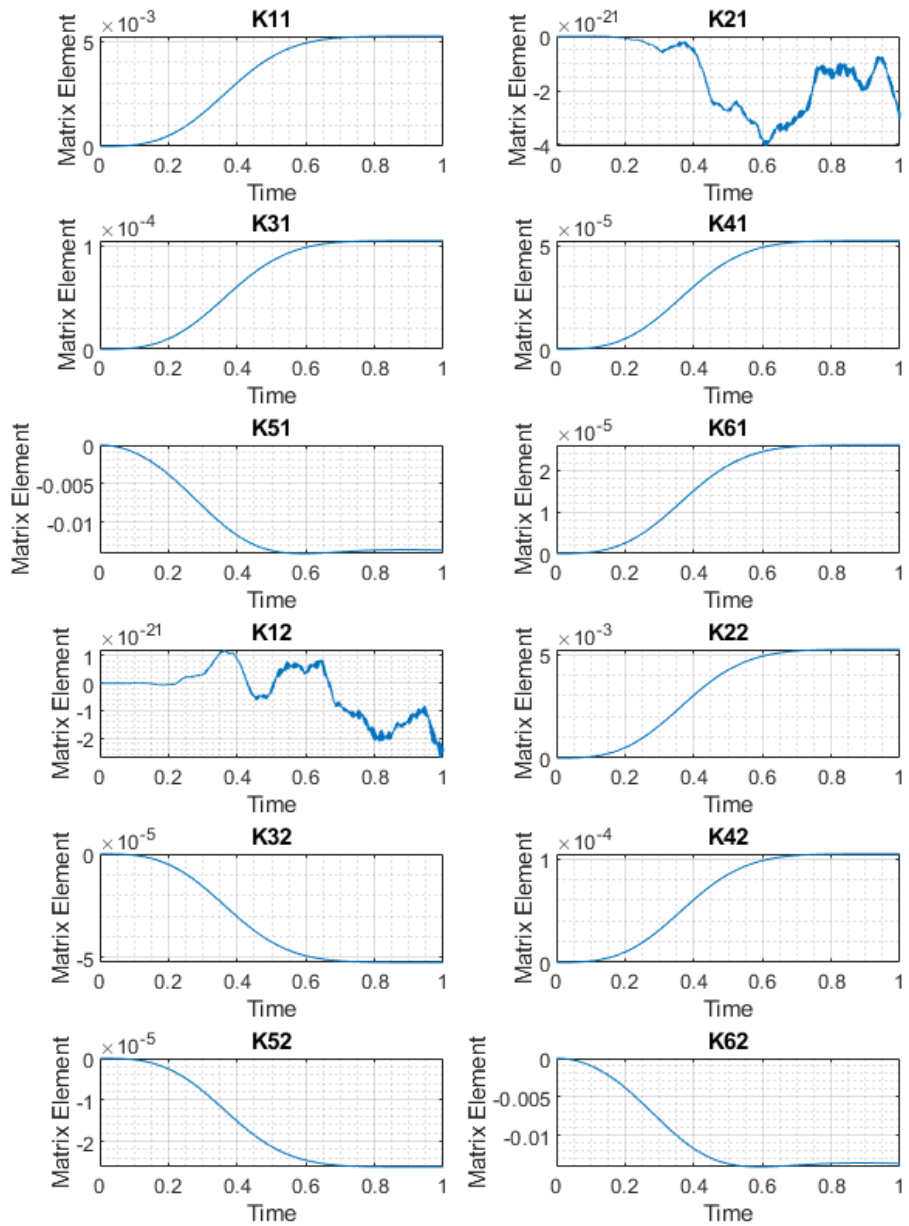
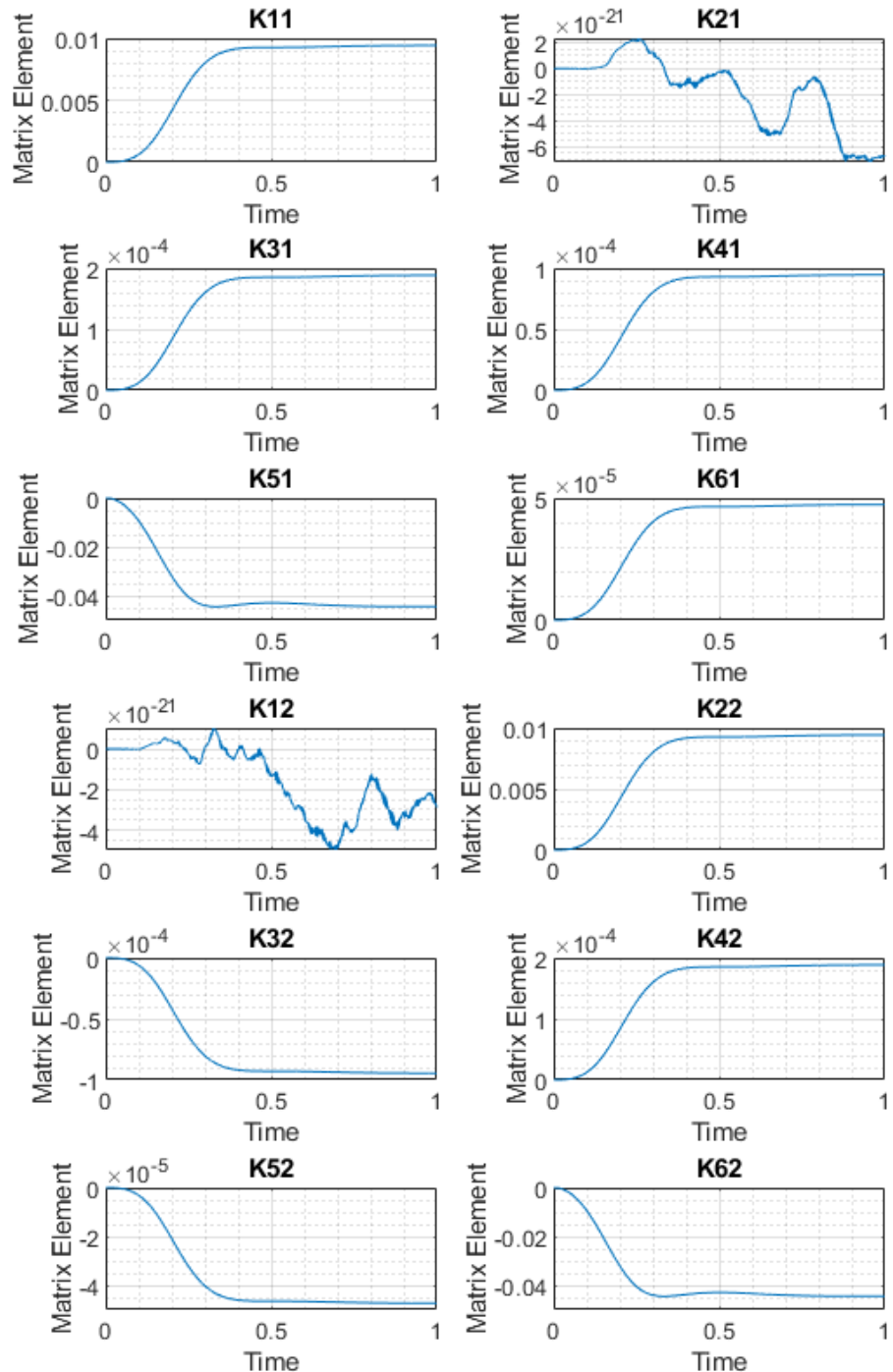


Figure 13: Time Evolution of Gains for SNR = 0.2



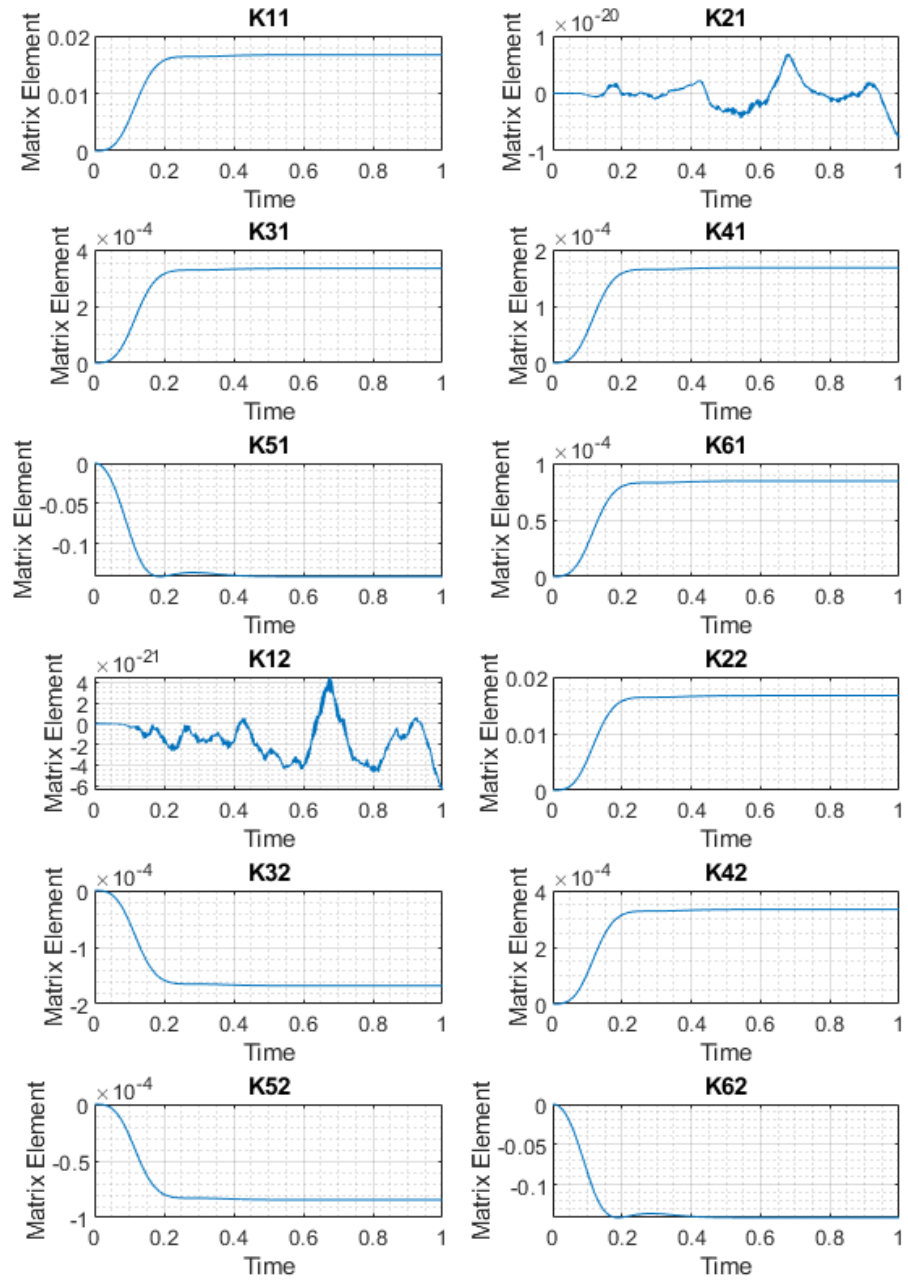


Figure 15: Time Evolution of Gains for SNR = 20

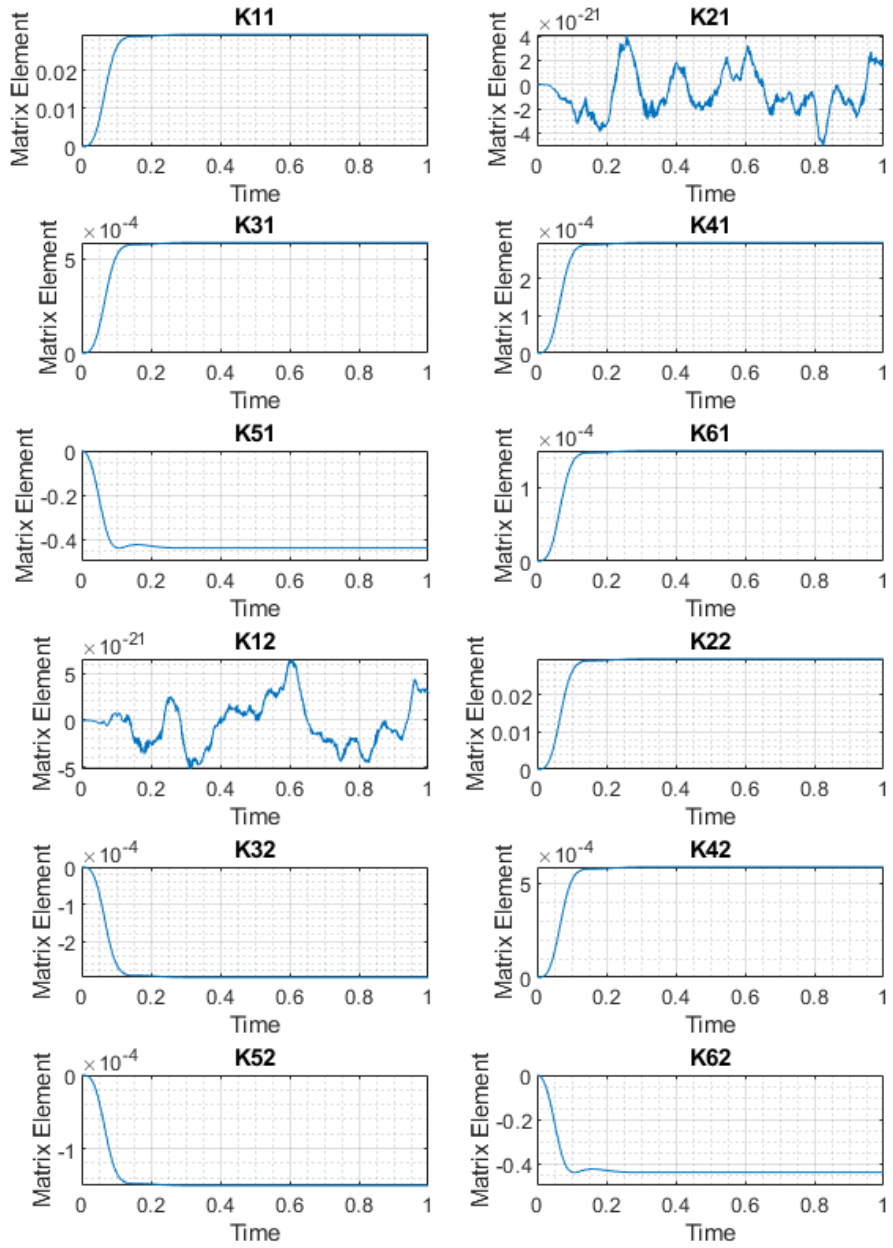


Figure 16: Time Evolution of Gains for SNR = 200

### 1.3 Simulating for different $P_0$ matrix

We choose a much smaller  $P_0$  matrix for the next set of simulations.

$$P_0 = \begin{pmatrix} 0.05 & 0 & 0 & 0 & 0 & 0 \\ 0 & 0.05 & 0 & 0 & 0 & 0 \\ 0 & 0 & 0.05 & 0 & 0 & 0 \\ 0 & 0 & 0 & 0.05 & 0 & 0 \\ 0 & 0 & 0 & 0 & 0.05 & 0 \\ 0 & 0 & 0 & 0 & 0 & 0.05 \end{pmatrix}$$

#### 1.3.1 Variation of $\delta_x$

We observe that despite large measurement noise from the sensor data, the state estimate is very close to the true state. The power of Kalman filtering algorithm is depicted clearly here.

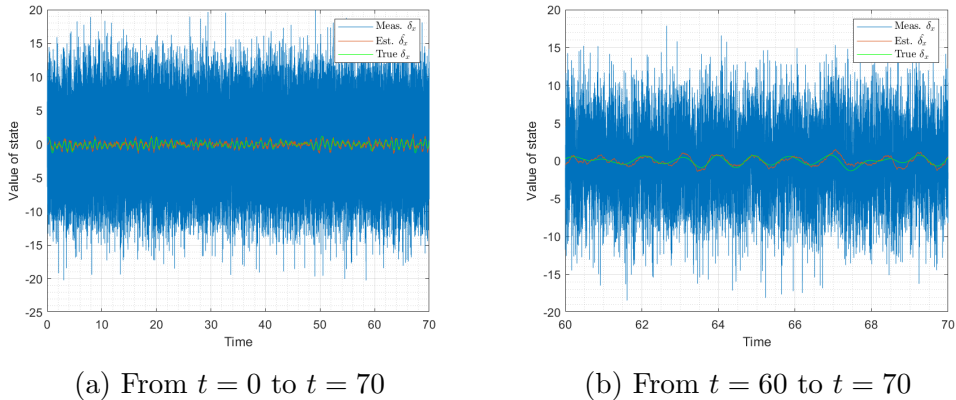


Figure 17: For Signal-to-Noise Ratio = 0.2

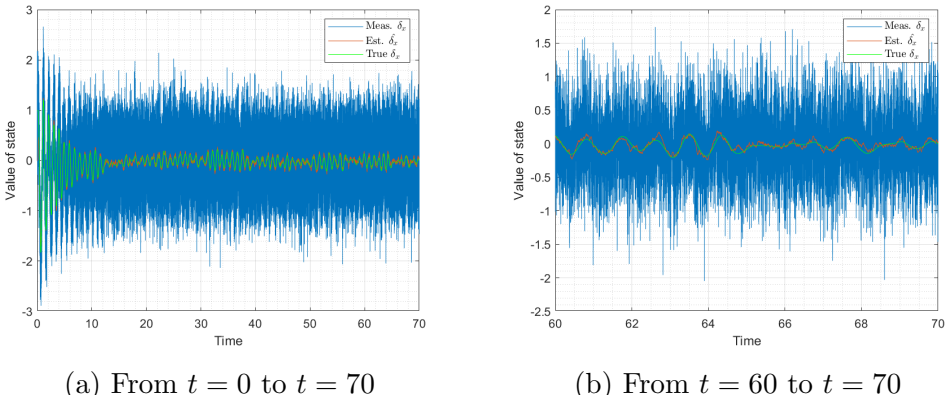


Figure 18: For Signal-to-Noise Ratio = 2

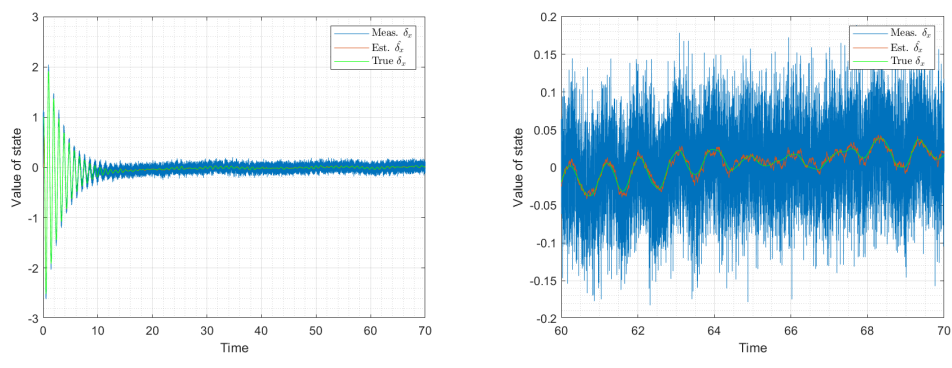


Figure 19: For Signal-to-Noise Ratio = 20

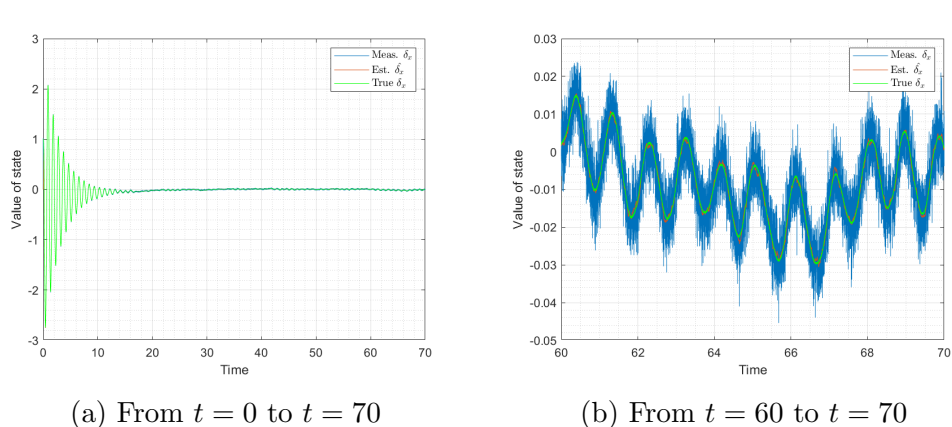


Figure 20: For Signal-to-Noise Ratio = 200

The blue line is for the measurement, and the orange line is for the estimated state, and the green line is for the true state.

### 1.3.2 Variation of $\delta_y$

We observe that despite large measurement noise from the sensor data, the state estimate is very close to the true state. The power of Kalman filtering algorithm is depicted clearly here.

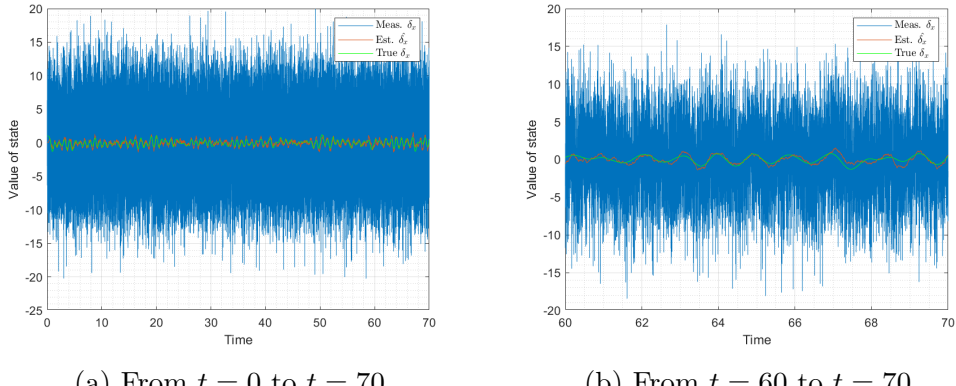


Figure 21: For Signal-to-Noise Ratio = 0.2

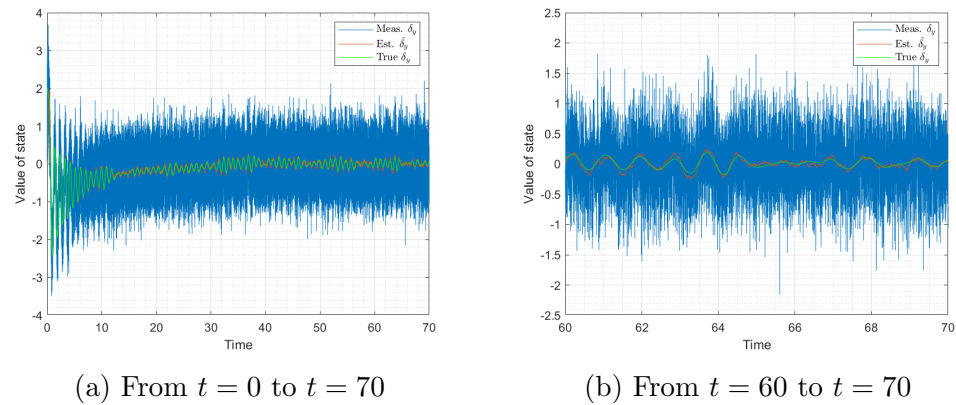


Figure 22: For Signal-to-Noise Ratio = 2

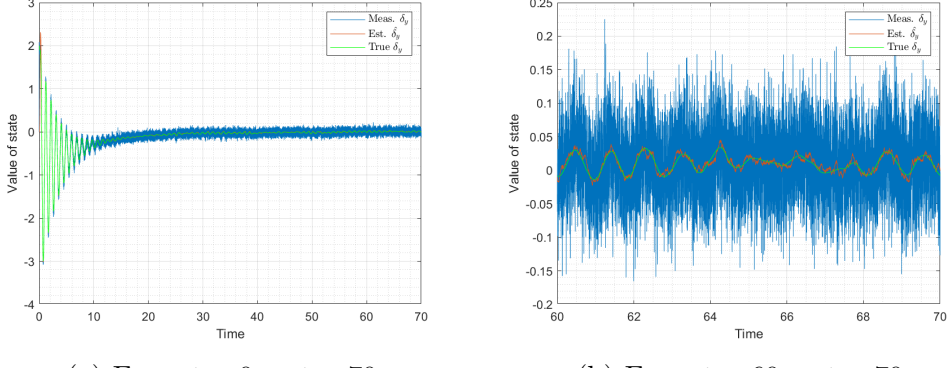
(a) From  $t = 0$  to  $t = 70$ (b) From  $t = 60$  to  $t = 70$ 

Figure 23: For Signal-to-Noise Ratio = 20

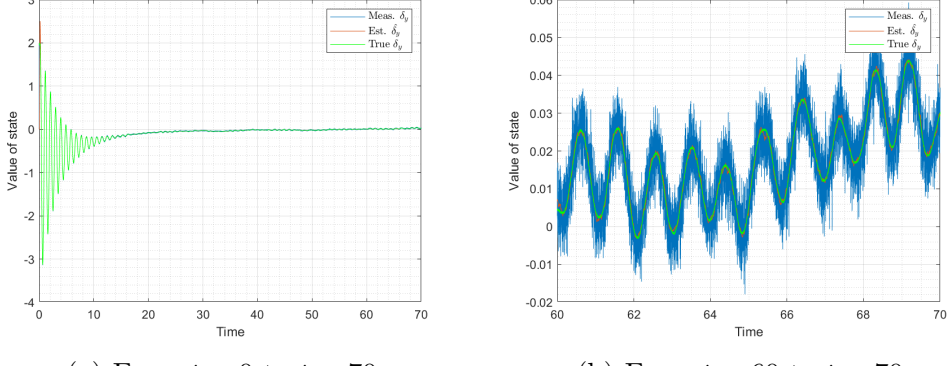
(a) From  $t = 0$  to  $t = 70$ (b) From  $t = 60$  to  $t = 70$ 

Figure 24: For Signal-to-Noise Ratio = 200

The blue line is for the measurement, and the orange line is for the estimated state, and the green line is for the true state.

We observe that variation of the initial  $P_0$  matrix does not have much dependence as time progresses. The dependence is just on the initial adaption to the estimates.

## 2 Question 2: Autopilot Missile

### 2.1 Controller Design

From the analysis presented earlier, we see that as the system is already stable, one needs to send appropriate control input  $u$  corresponding to the

commanded normal acceleration ( $a_{NC}$ ). The following controller is used:

$$u = \frac{M_\alpha}{M_\alpha \cdot Z_\delta - M_\delta \cdot Z_\alpha} \cdot a_{NC}$$

## 2.2 Simulating the system

The system is simulated for initialization of:

$$P_0 = \begin{pmatrix} 100 & 0 & 0 \\ 0 & 100 & 0 \\ 0 & 0 & 100 \end{pmatrix}$$

The initial state is  $x_0 = [1, 2, 1]^T$ , however the initial estimate of the state is  $[0, 0, 0]$ .

### 2.2.1 Interesting Plots

For the case when  $a_{NC} = 1000 \text{ ft/s}^2$ , we set the variance of the process noise and measurement noises to be 0.1. The following plots are obtained.

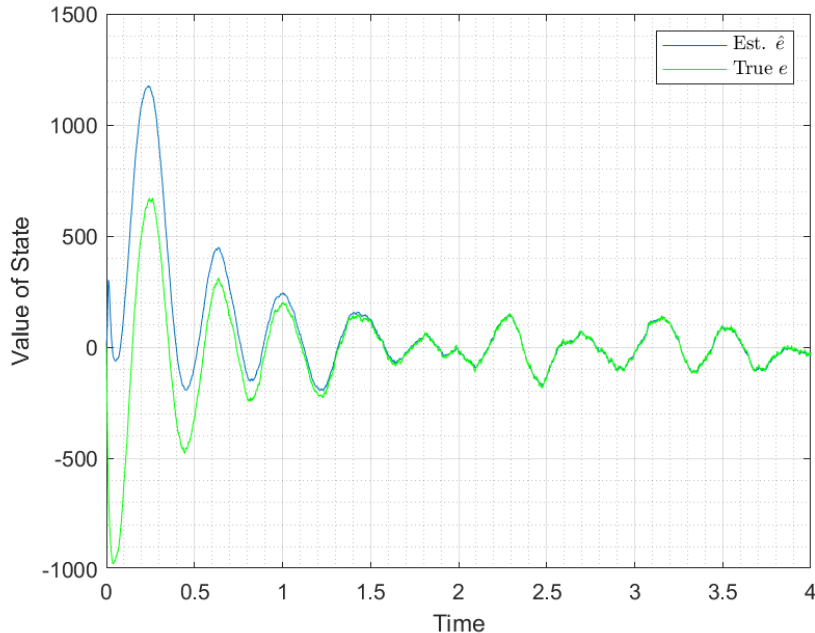


Figure 25: Variation of the state  $e$

The estimate converges and but still there are oscillations due to the process noise.

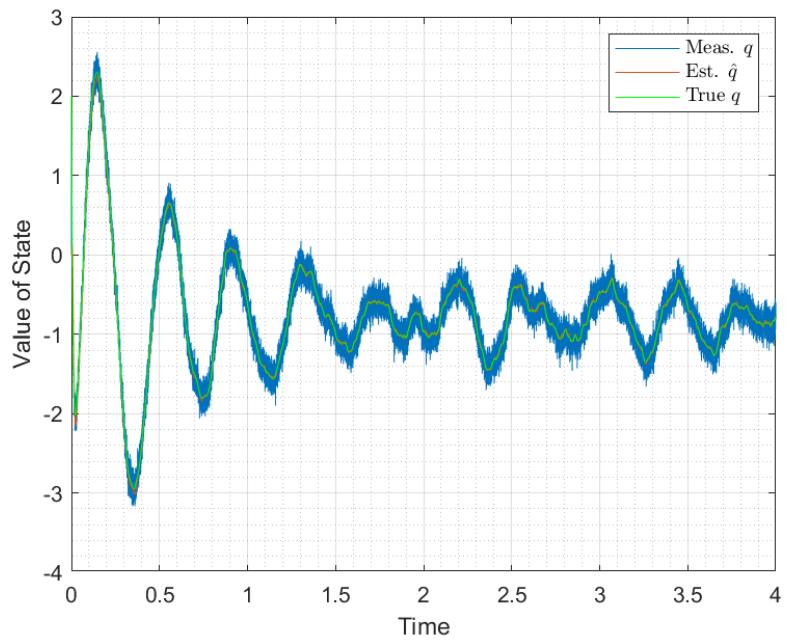


Figure 26: Variation of the state  $q$

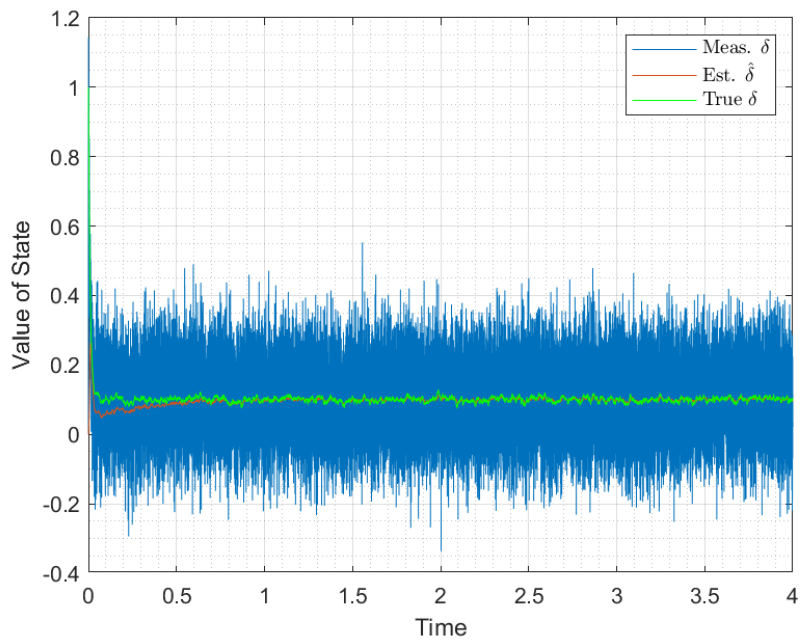


Figure 27: Variation of the state  $\delta$

Despite decently large measurement noise, the estimates are much closer to the true state.

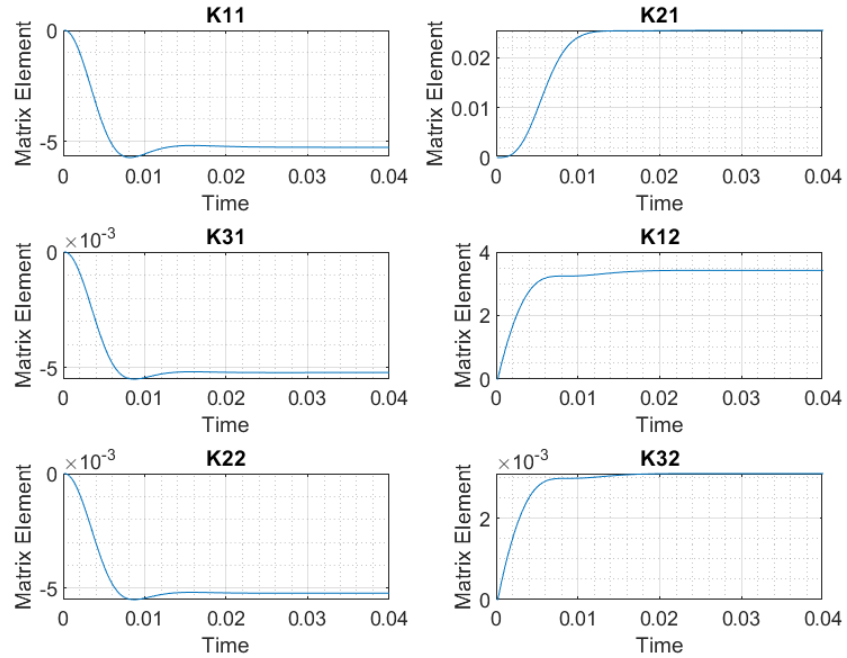


Figure 28: Variation of the elements of the Kalman gain matrix

The Kalman filter elements converge to the steady state value very soon, as seen in the above plots. They have different rates of convergence as decided by the eigenvalues.

### 2.2.2 Variation of states for $V/W_g = 1000, V/W_a = 1$

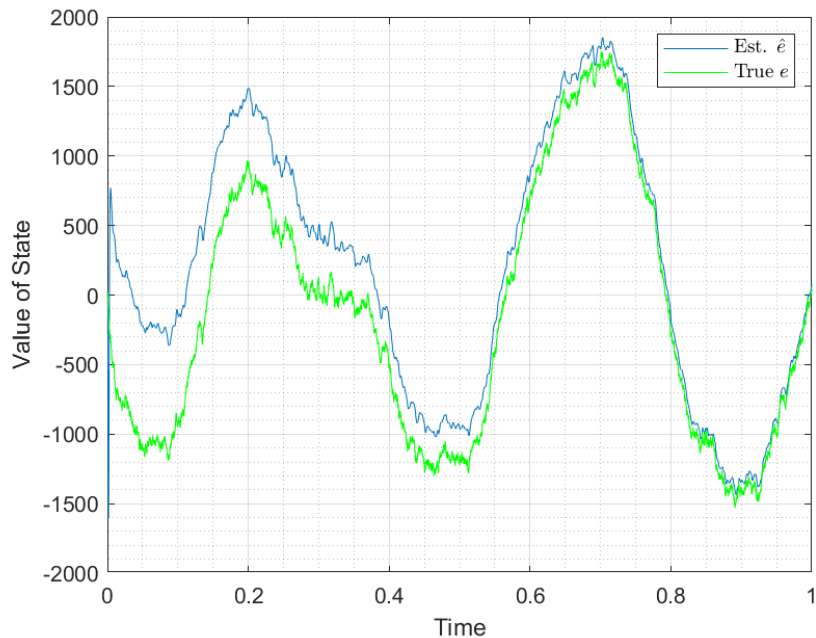


Figure 29: Variation of the state  $e$

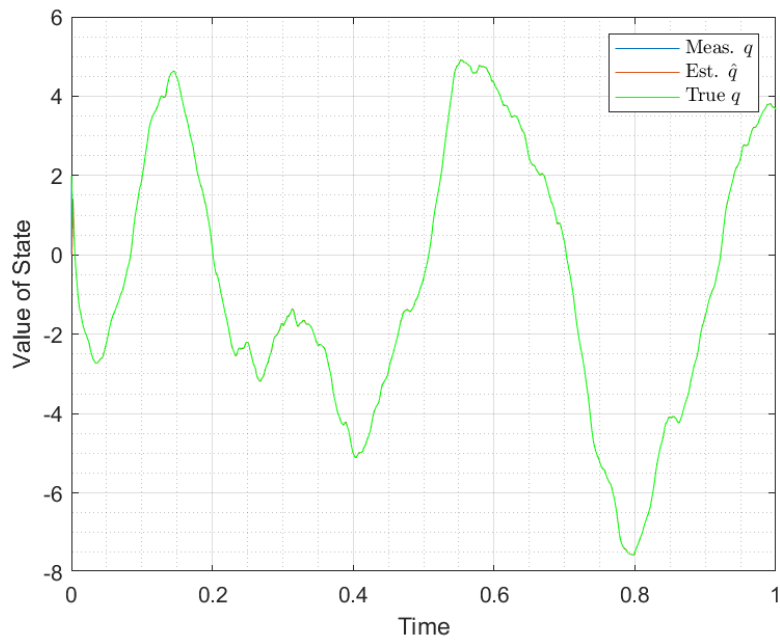


Figure 30: Variation of the state  $q$

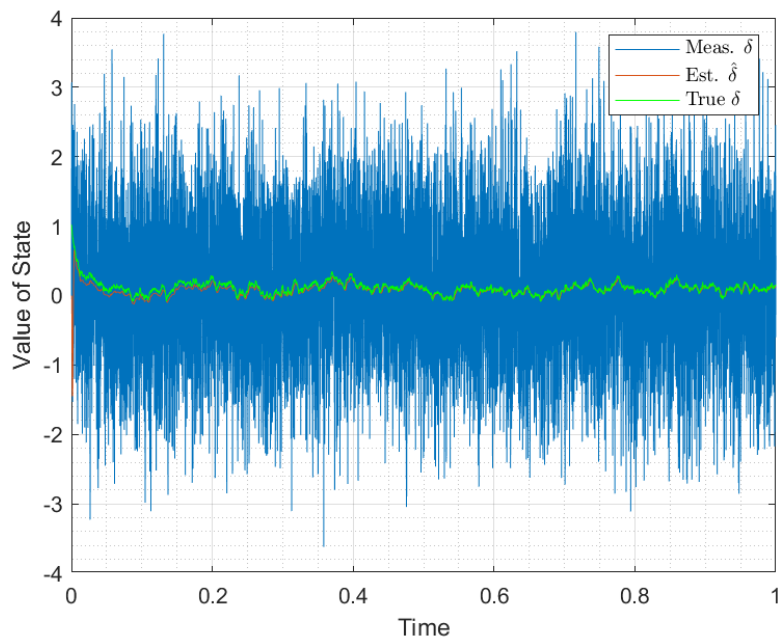


Figure 31: Variation of the state  $\delta$

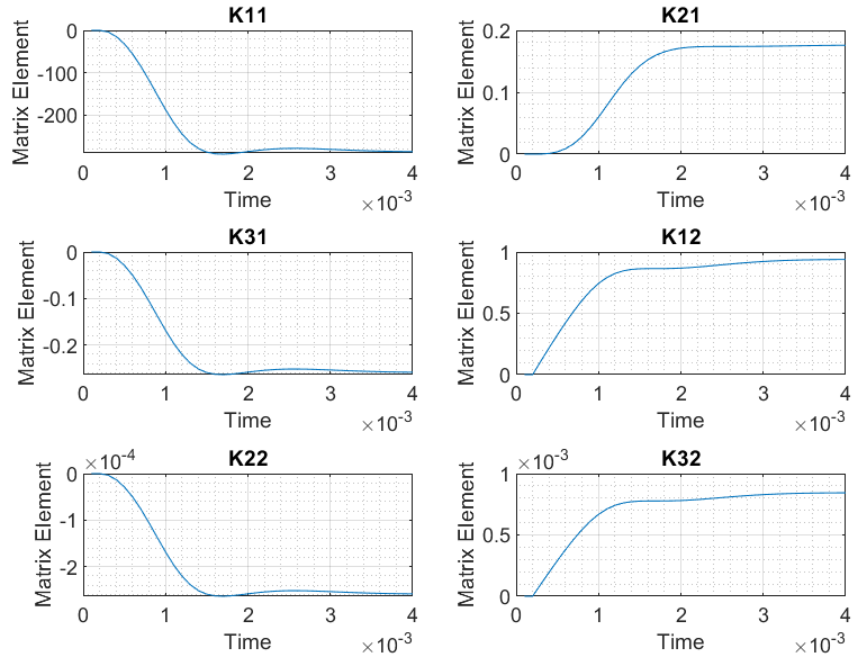


Figure 32: Variation of the elements of the Kalman gain matrix

Similar observations as before. The noise in the  $\delta$  is higher; still, the estimates are very close. The process noise has been increased 10-fold in this simulation; hence we see larger oscillations in the plot of  $e$ .

### 2.2.3 Variation of states for $V/W_g = 1, V/W_a = 1000$

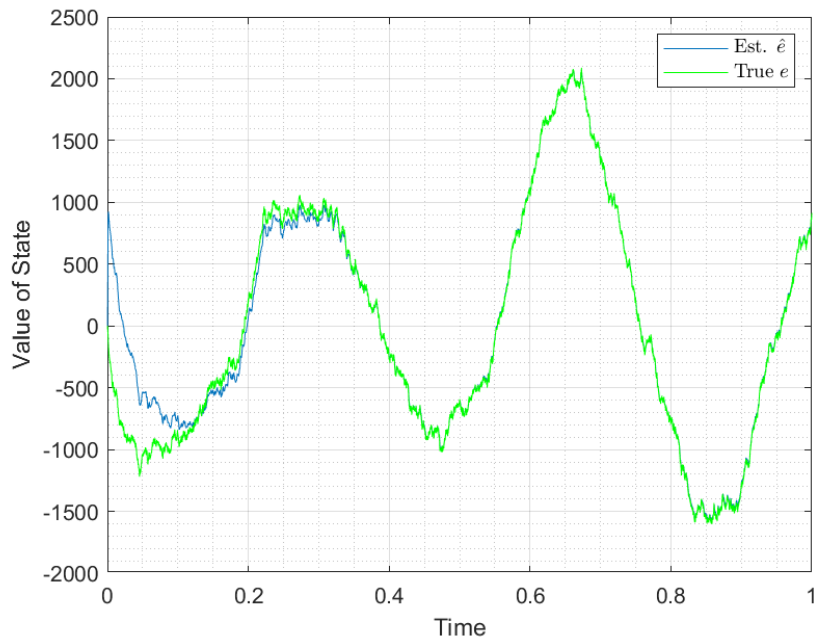


Figure 33: Variation of the state  $e$

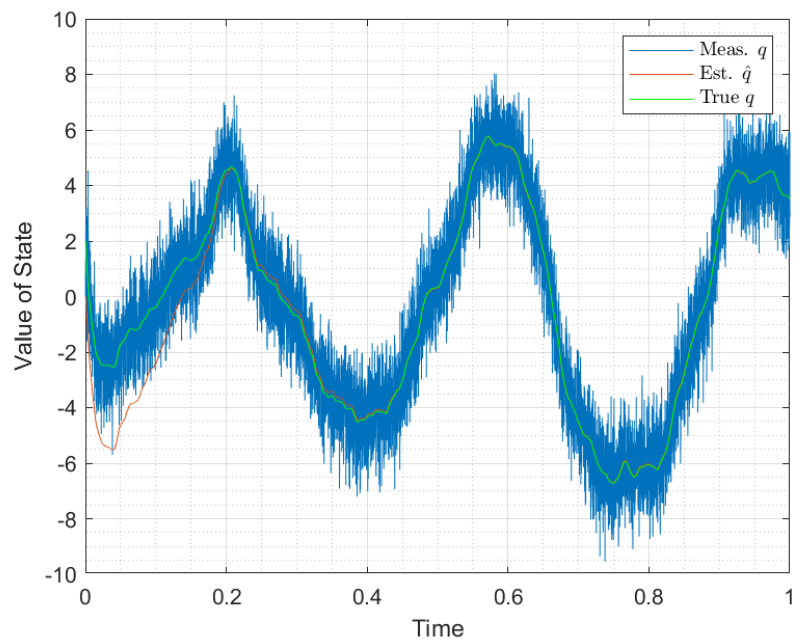


Figure 34: Variation of the state  $q$

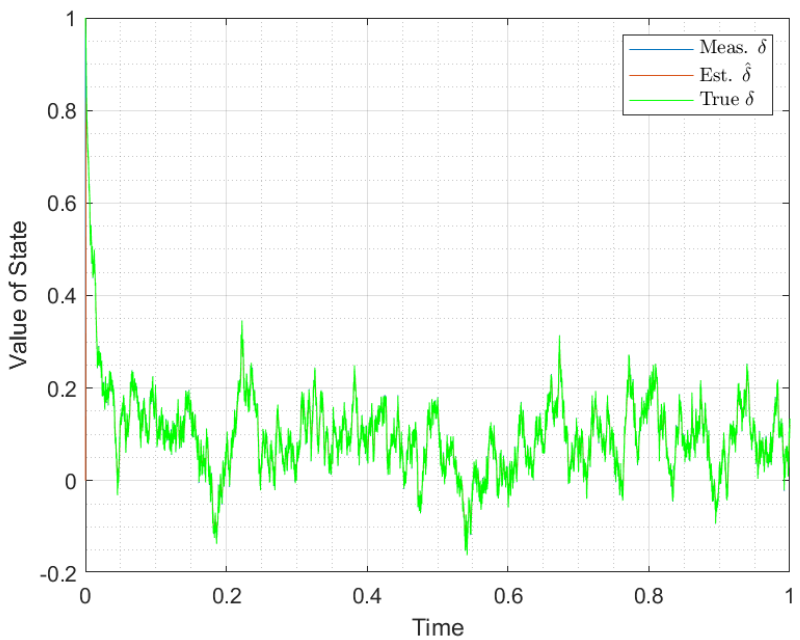


Figure 35: Variation of the state  $\delta$

Similar observations as before. The noise in the  $q$  is higher; still, the estimates are very close. The process noise has been increased 10-fold in this simulation; hence we see larger oscillations in the plot of  $e$ .

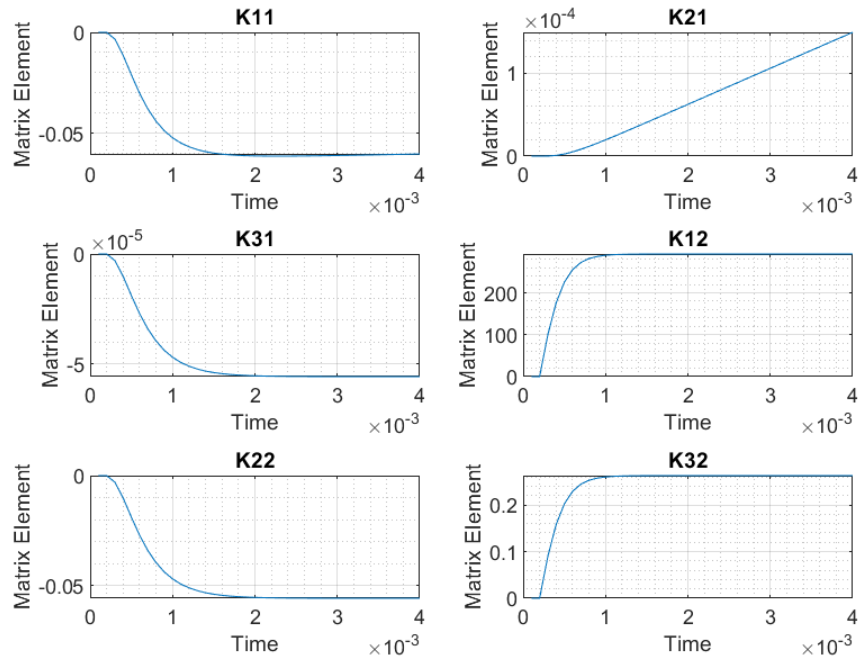


Figure 36: Variation of the elements of the Kalman gain matrix for a smaller time scale

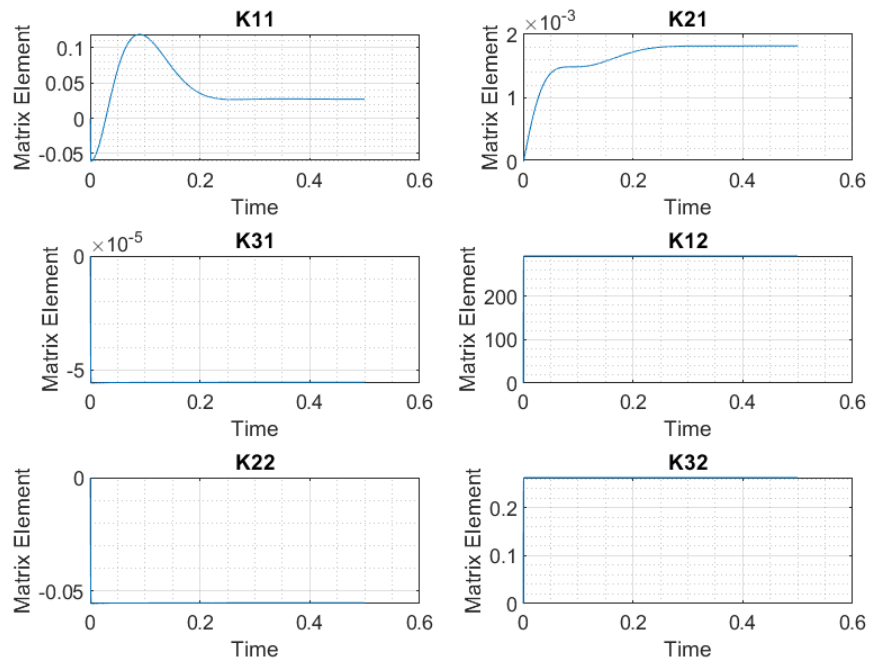


Figure 37: Variation of the elements of the Kalman gain matrix for a longer time scale

Some of the elements in the gain matrix converge much faster. This can be attributed to the fact that there is large noise in the other state.